THE GEOLOGY AND PALEONTOLOGY OF COGLAN BUTTES, OREGON

by

KRISTEN ANTOINETTE MᴀᴄKENZIE

A THESIS

Presented to the Department of Geological Sciences
and the Graduate School of the University of Oregon
in partial fulfillment of the requirements
for the degree of
Master of Science

June 2013

THESIS APPROVAL PAGE

Student: Kristen Antoinette MacKenzie

Title: The Geology and Paleontology of Coglan Buttes, Oregon

This thesis has been accepted and approved in partial fulfillment of the requirements for the Master of Science degree in the Department of Geological Sciences by:

Dr. Samantha S.B. Hopkins	Chair
Dr. Rebecca J. Dorsey	Member
Dr. David P. Whistler	Member

and

Kimberly Andrews Espy	Vice President for Research & Innovation/Dean of the Graduate School

Original approval signatures are on file with the University of Oregon Graduate School.

Degree awarded June 2013

THESIS ABSTRACT

Kristen Antoinette MacKenzie

Master of Science

Department of Geological Sciences

June 2013

Title: The Geology and Paleontology of Coglan Buttes, Oregon

The outcrops of Coglan Buttes in southern Oregon are composed of numerous distinct sedimentary sandstone and volcaniclastic beds. In the past it has been mapped as a single Miocene sedimentary unit. Though the area was known to have produced vertebrate fossils, they had not been studied. My research presented here is the first in-depth study of both the geology and the paleontology of the area. The 620 meters of interbedded sandstones, pyroclastic deposits and volcanic sheet flows change in lateral thickness; they indicate significant paleotopography.   In addition I describe the vertebrate assemblages contained within these geologic units and compare them with other North American assemblages. The Coglan Buttes faunas share affinity to those of the John Day Basin assemblages in part, as well as with southern latitude faunas of California, Florida and Texas. The faunal composition of the Coglan Buttes assemblage indicates an earliest Miocene (late Arikareean) age.

CURRICULUM VITAE

NAME OF AUTHOR: Kristen Antoinette MacKenzie

GRADUATE AND UNDERGRADUATE SCHOOLS ATTENDED

University of Oregon, Eugene, OR
University of Idaho, Moscow, ID
Walla Walla University, College Place, WA
Whitman College, Walla Walla, WA
Walla Walla Community College, Walla Walla, WA

DEGREES AWARDED:

Master of Science, Geology, 2013, University of Oregon
Bachelor of Science, Biology, 1999, Walla Walla University

AREAS OF SPECIAL INTEREST:

Vertebrate Paleontology/Biostratigraphy, Sedimentary Geology, Museum
Curation

PROFESSIONAL EXPERIENCE:

Museum Technician, John Day Fossil Beds National Monument, 2012

Graduate Teaching Fellow, Department of Geological Sciences, University of
Oregon, 2011-2013

Curation Assistant, Condon Collection, Museum of Natural and Cultural History,
Department of Geological Sciences, University of Oregon, 2011-2013

GRANTS, AWARDS, AND HONORS:

Ewart Baldwin Fellowship, Museum of Natural and Cultural History, University
of Oregon, 2011-2012

Johnston Scholarship, University of Oregon, Department of Geological Sciences,
2012

Graduate Teaching Fellowship, Geological Sciences, 2011 to present

ACKNOWLEDGMENTS

TABLE OF CONTENTS

LIST OF FIGURES

LIST OF TABLES

CHAPTER I

INTRODUCTION

Coglan Buttes, Oregon (Fig. 1) is in the northwestern Basin and Range, a physiographic province of normal faults resulting from crustal extension. The southwest-facing hills of Coglan Buttes are primarily mafic volcanic flows of uncertain age. Directly to the southeast of the summit, over 400 meters (m) of interbedded sedimentary rocks, volcaniclastics and volcanic flows are exposed along a northwest-southeast trend. These deposits are mapped as a single sedimentary unit in a 1963 United States Geological Survey Map (USGS)(Walker, 1963). The sedimentary outcrops produce a diverse assemblage of vertebrate fossils. Though Walker's 1963 map identifies several locations in the Coglan Buttes vicinity known to produce vertebrate fossils, they have not been studied previously. Walker (1963) assigns a Miocene age, 23.8-5.3 million years (Ma), to the sedimentary beds. However, vertebrate paleontologists further subdivide geological epochs into North American Land Mammal (NALMA) ages. NALMA ages are biostratigraphic units based on faunal assemblages found within distinct biozones and are usually supported with radiometric dates (Woodburne, 2004a). A more accurate age of the Coglan Buttes outcrops may be determined based on the vertebrate fossils they contain rather than the previous estimate that spans 18.5 million years.
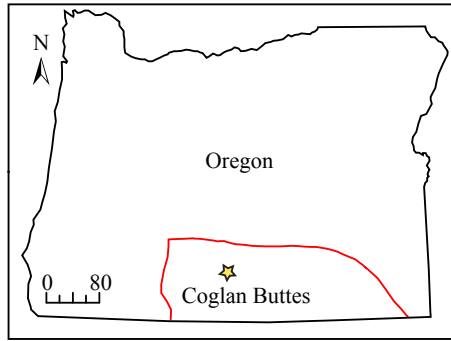
Figure 1. Location of Coglan Buttes, Oregon. Scale is in kilometers, red line indicates northwestern extent of the Basin and Range physiographic province within Oregon.

Geological Context

There has been little comprehensive geologic work done in the immediate vicinity of Coglan Buttes (Lake County, Or). United States Geological Survey (USGS) employees, Walker (1963), and Peterson and McIntyre (1970), mapped the area. They were mainly interested in the mineral resources of Lake County, Oregon. Peterson and McIntyre (1970) discuss the Oligocene andesitic flows that underlie the fossiliferous deposits of Coglan Buttes but they do not discuss the fossil bearing rocks. Without citing the radiometric method used, Peterson and McIntyre (1970) indicate an age 33.1 Ma, +/- 1 Ma for the underlying andesite. Coglan Buttes is mapped as the same sedimentary, tuffaceous sandstones and pyroclastic units that are found about 45 kilometers south at Thomas Creek (Fig. 2), referred to as the "Paisley Hills" in older literature (now part of the Fremont-Wynema National Forest) (Peterson and McIntyre, 1970, Walker, 1963). The sedimentary units at Thomas Creek contain a Miocene fossil flora and an early Miocene rhinocerotid molar was found there (Peterson, 1959 and Peterson and McIntyre, 1970).

Recent geological work in the region by Scarberry et al. (2009) focused on an area just 10 kilometers east of Coglan Buttes in the Coleman Hills (Fig. 2). Scarberry et al. (2009) were investigating the timing of the extensional fault that formed Abert Rim. In the process they discovered the Coleman Hills to be an eroded early Miocene composite volcano with on-lapping volcaniclastic sedimentary beds bisected by a 22 Ma dike (Scarberry et al., 2009). Direct physical correlation of the Coglan Buttes rocks with the Coleman Hills is impossible; they are not contiguous. Furthermore, Scarberry et al. (2009) suggest the surrounding paleotopographic relief was 500 m or more.

Paleontology Context

In the earliest Miocene, much of Oregon was temperate; well-drained soils, open woodlands and plenty of water supported a rich plant and animal community (Retallack et al., 2000). Open woodlands still persisted near waterways through the middle Miocene, while grassy savannas developed elsewhere as a result of increasing aridity (Stromberg, 2004; Woodburne, 2004b). The changing landscape provided variable habitat that sustained ever-increasing diversification of fauna and flora through the Miocene (Woodburne, 2004b). While the rest of the early Miocene North American faunal assemblages show fairly strong similarities, central Oregon and western Idaho assemblages indicate distinct zoogeographical regions (Woodburne, 2004b). Early to early-middle Miocene localities are rare throughout the western states, restricted mostly to the John Day Basin of Oregon, west of the Continental Divide in Montana and Idaho and in the Mojave Desert of the southern Great Basin (Woodburne et al., 2004).

Figure 2. Coglan Buttes relative to Paisley, Oregon. The blue rectangle is the extent of Fig. 3, yellow star is the location of Paisley, Oregon and the yellow oval is the extent of the Thomas Creek fossil locality. State Highways (Hwy) and Oregon State roads for reference.

The well-known fossiliferous deposits of the John Day Basin contain some of the best fossil records of the Eocene-Miocene (Woodburne, 2004; Fremd, 2010). However its most productive Arikareean (latest Oligocene-early Miocene) sites are restricted to one section of the John Day Formation, the Turtle Cove Member (TCM; Fremd, 2010; Woodburne, 2004). The TCM early Arikareean units are exceptionally productive but the latest Arikareean contains a less well-preserved fauna (Fremd, 2010). Late Arikareean fossiliferous beds are also found in the Kimberly Member, Haystack Valley Member, Johnson Canyon Member and Balm Creek Member of the John Day Basin (Hunt and Stepleton, 2004), but the fossil sites in these parts of the John Day Formation are a great deal less productive than the TCM. Unlike the latest Arikareean deposits of the John Day Basin, the Coglan Buttes site produces a diverse, well-preserved macro- and microfauna. Many *in situ* specimens are partially articulated cranial and associated postcranial elements.

Walker's 1963 map indicates three locations within the Coglan Buttes area known to contain vertebrate fossils. There is no formal documentation of fossil collection efforts. The Museum of Natural and Cultural History (MNCH), University of Oregon (UO) does have a few fossils that may have come from the area; they are labeled with place names from the surrounding area but lack contextual data or field notes. It is likely that Peterson collected them, as he is the only geologist known to document fossil locations within the Coglan Buttes area (Walker 1953, Peterson and McIntyre, 1970). However, absent documentation of the provenance of this material, its origin remains speculative.

CHAPTER II

METHODS

Geology Methods

After discovering fossil material at the Coglan Buttes site in 2006, I worked to find the local extent of the fossil-bearing beds across six miles of northwest-to-southeast-trending exposures immediately southeast of Coglan Buttes. I have focused on four areas that have high concentrations of vertebrate fossils (Fig. 3). These four areas will be referred to as Guzzler, Beardog, Shelter and Mylagaulid. The section names are given to areas of relatively high fossil concentration and reflect items found there; they are not standardized USGS place names. At each of these sites I measured and described the stratigraphy. A Brunton compass was used to record bedding strike and dip. The dip is consistent throughout the outcrops; it varied between 4°-7° and I used 5.5° as the dip while measuring columnar sections. I used a Jacobs staff and Abney level (set to 5.5°) to measure bed thicknesses and described the lithology of each distinctive layer. I produced geologic maps for each of these areas (Figs. 4-7). The maps were drafted in ArcGIS to allow future revisions of data layers as necessary. These geologic maps also contain locations of stratigraphic columns and University of Oregon (UO) fossil localities. UO fossil locality numbers are assigned to areas within a single bed layer and have natural boundaries that are visible on the ground such as drainages, a cliff face and distinct ridges.
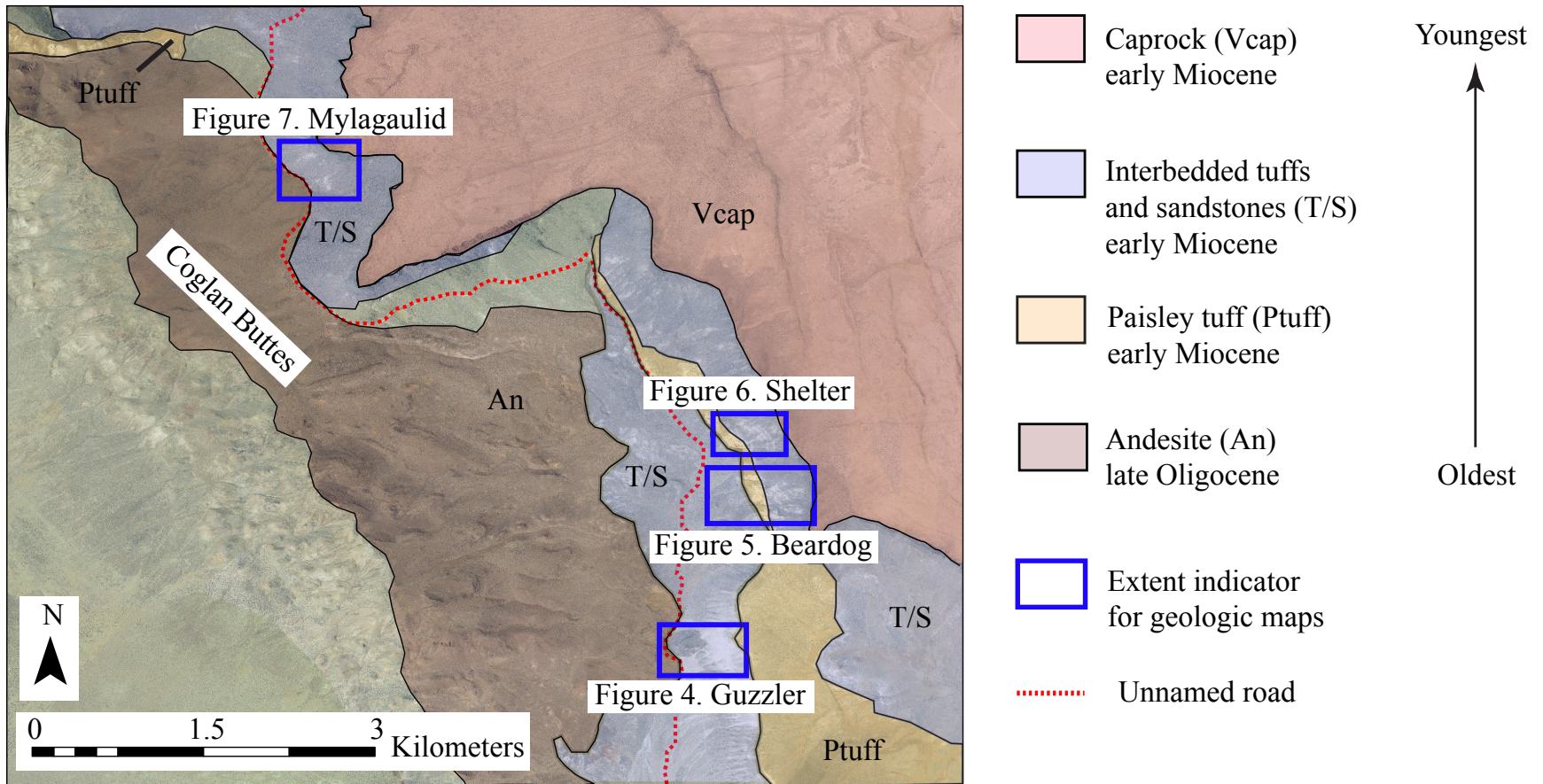
Figure 3. General geology of Coglan Buttes. Base Image: Oregon Imagery Explorer
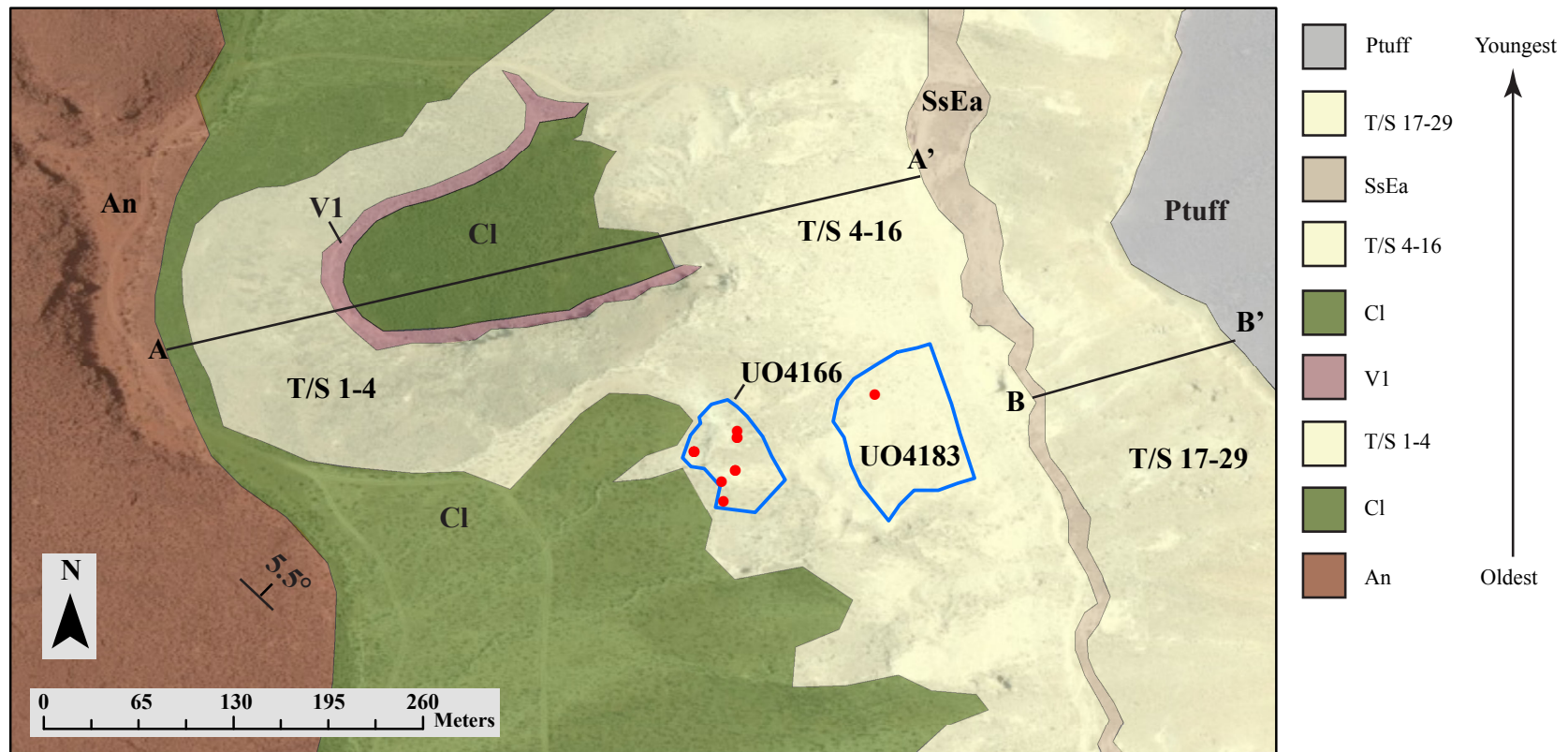
Figure 4. Geologic map for Guzzler area. Abbreviations and colors are carried through to the corresponding stratigraphic column (Fig. 8) and are defined in Table 2. Solid black lines labeled A-A' and B-B' are the routes taken while measuring the stratigraphy. Red dots are fossil locations, blue polygons are UO localities. Base Image: ESRI, Projection: Lambert Conformal Conic, Coordinate System: NAD 1983 Harn Oregon Lambert Feet Intl.
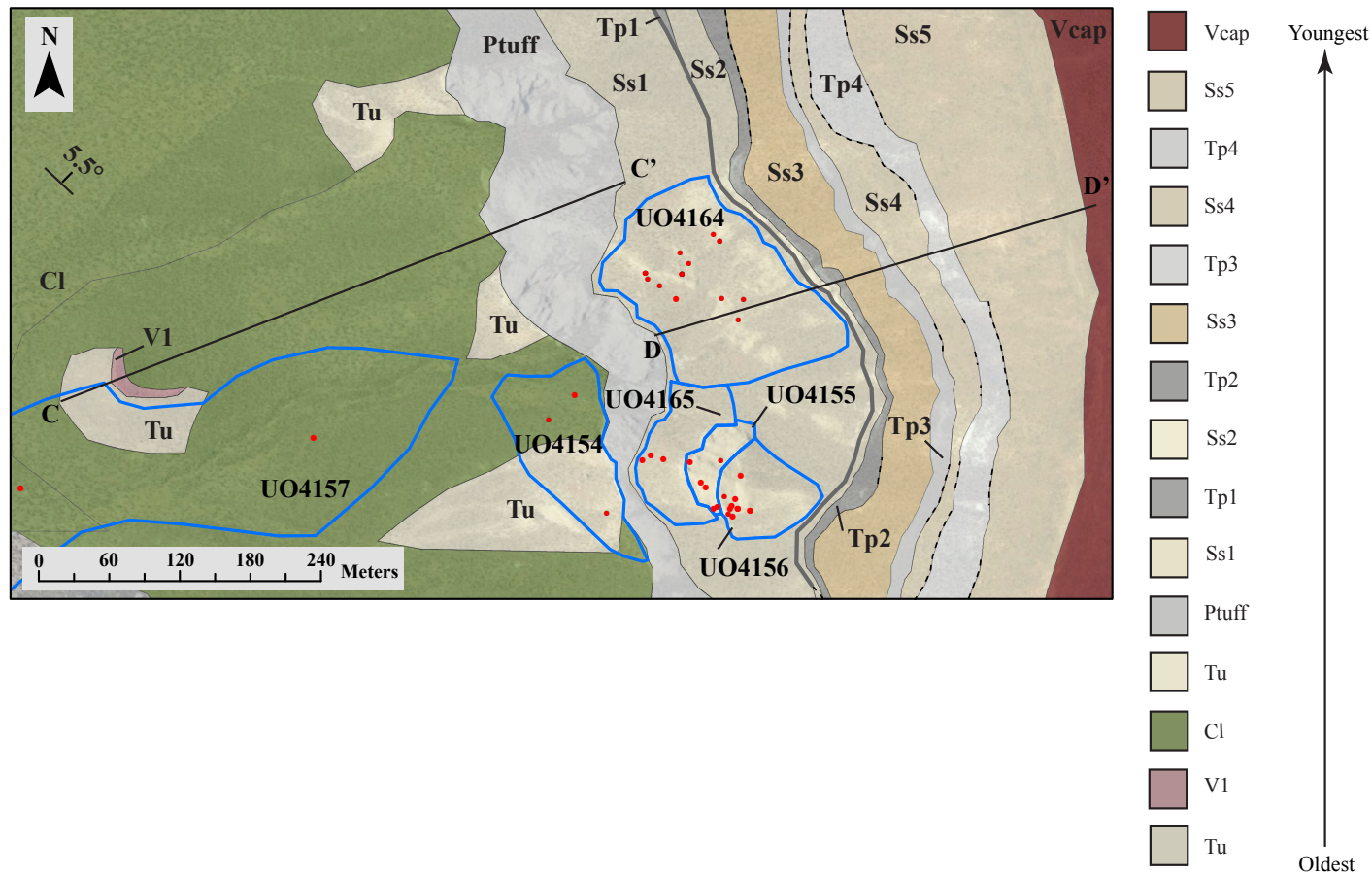
Figure 5. Geologic map for Beardog area. Stratigraphic unit abbreviations are the same for the corresponding stratigraphic column (Fig. 9) and are defined in Table 2. Solid black lines labeled C-C' and D-D' are the routes taken while measuring the stratigraphy. Red dots are fossil locations, blue polygons are UO localities and dashed heavy lines are inferred contacts. Base Image: ESRI, Projection: Lambert Conformal Conic, Coordinate System: NAD 1983 Harn Oregon Lambert Feet Intl.
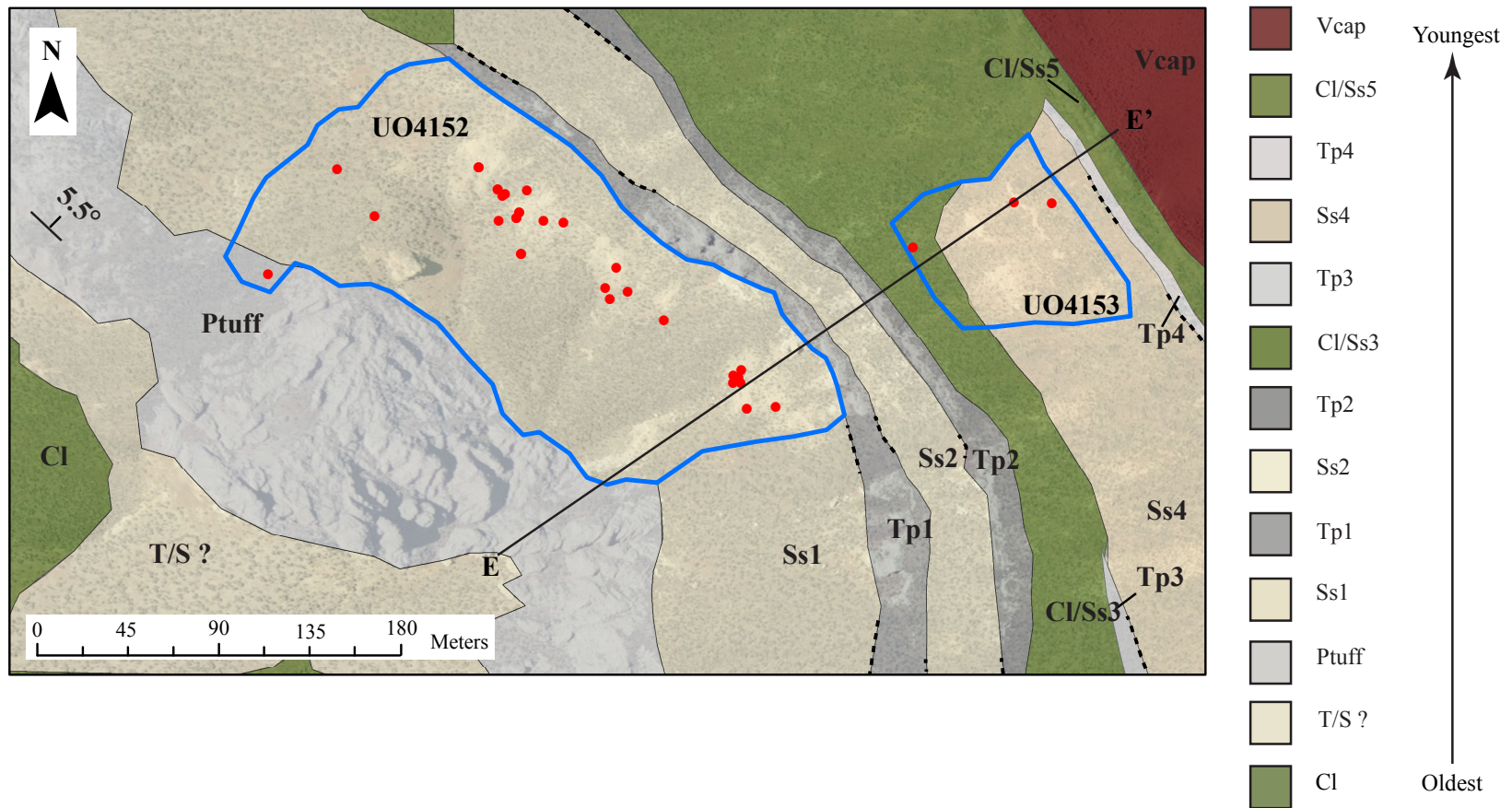
Figure 6. Geologic map for Shelter area. Stratigraphic unit abbreviations and colors are the same for the corresponding stratigraphic column (Fig. 10) and are defined in Table 2. Solid black line labeled E-E' is the route taken while measuring the stratigraphy. Red dots are fossil locations, blue polygons are UO localities, and heavy dashed lines are inferred contacts. Base Image: ESRI, Projection: Lambert Conformal Conic, Coordinate System: NAD 1983 Harn Oregon Lambert Feet Intl.
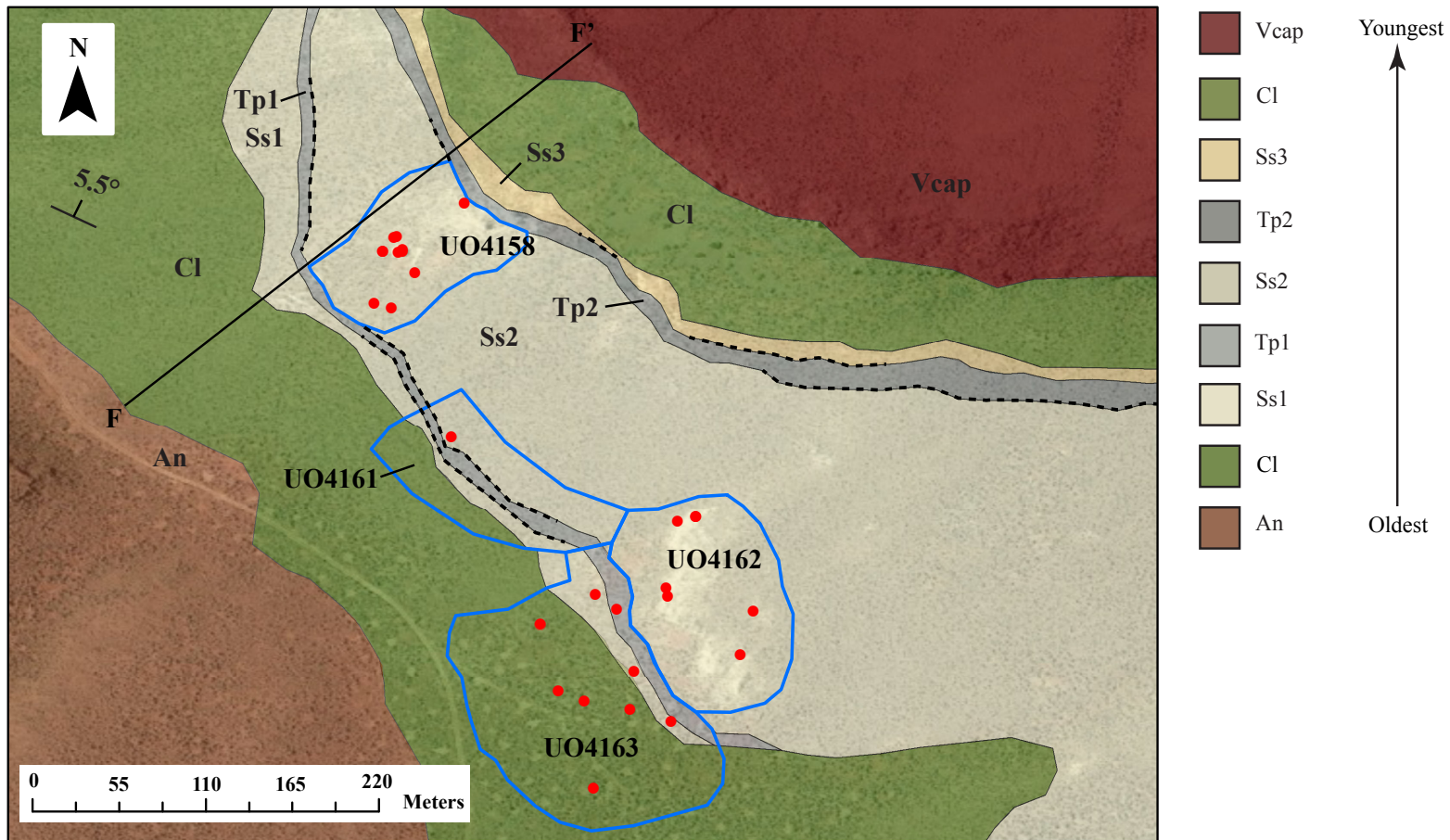
Figure 7. Geologic map for Mylagaulid area. Stratigraphic unit abbreviations and colors are same for the corresponding stratigraphic column (Fig. 11) and are defined in Table 2. Solid black line labeled F-F' is the route taken while measuring the stratigraphy. Red dots are fossil locations, blue polygons are UO localities and heavy dashed lines are inferred contacts.
Base Image: ESRI, Projection: Lambert Conformal Conic Coordinate System: NAD 1983 Harn Oregon Lambert Feet Intl.

Radiometric dating of several key lithologic units is as yet unfinished, pending

further analysis at the Oregon State University Argon Geochronology Laboratory. The

rock units I chose for dating were found to contain high amounts of sanidine (high

temperature form of potassium feldspar), biotite and plagioclase-feldspars. Sanidine is

ideally suited for $^{40}Ar/^{39}Ar$ analysis and is considered to yield the most precise dates for

terrestrial volcanic rocks (Renne et al., 1994). I collected three samples for dating: 1) the

capping ash Tp2 from the Mylagaulid section (Figs. 5-7), 2) Paisley tuff (Ptuff) (Figs. 4-

6) and 3) the lowest ash (T/S6) of the Guzzler section (Fig. 8). I chose Tp2 because it is

the first ash tuff that immediately caps the uppermost fossiliferous bed. Similarly, I

collected T/P6 because it is directly under the lowest fossil bearing unit in Guzzler

section. T/P 6 can be found throughout the southern end of the basin and is consistently

the same dark grey color and approximately the same thickness and grain size; it is

readily recognized. I chose the Paisley tuff because it is the single most recognizable

layer throughout the entire Coglan Buttes basin and elsewhere in Lake County west of

Coglan Buttes. I am informally naming the tuff until I can determine whether the unit

has been studied or named elsewhere in the region. The Paisley tuff will be crucial for

correlating any future paleontological or geological research in the region. The upper and

lower dates will provide age constraint on the fauna of Coglan Buttes. The coordinate

data for these samples is in Table 1.

Table 1. Coordinate data for samples obtained for radiometric dating. Datum is World
Geodetic System 84, Universal Transverse Mercator. Uncertainty is +/- 3-4 meters.

Unit	Zone	Easting	Northing
Tp2	10T	0716061	4726048
Ptuff	10T	0717950	4725059
T/P 6	10T	0718781	4721690

Paleontology Methods

Fossil collection was permitted under Bureau of Land Management (BLM) Permit OR-40510 and seasonal work authorizations were obtained from the Lakeview (OR, BLM) office. This permit is the John Day Fossil Beds National Parks permit, with oversight provided by Theodore Fremd (2009-2010) and Joshua Samuels (2010-present). All fossils collected are property of the Bureau of Land Management and have been formally accessioned (UO Acc. 2013.1) at the University of Oregon, Museum of Natural and Cultural History, Condon Collection (UOMNCH). All fossils described in this paper have a unique record in the museum's database and will be referred to as: UOMNCH F-####. Fossil coordinates were recorded with a handheld Global Positioning System: Garmin Etrex Legend Cx. Coordinate data for the fossils is on record with UOMNCH.

In an attempt to collect this new site comprehensively, I employed two methods: surface collection and screening of matrix and anthills for microfossils. Fossils were generally found in float, though many *in situ* specimens were located and noted for future excavation. Fossils found in float were assigned to the stratigraphic unit they were found.

Fossils found *in situ* were at first excavated with hand tools, after polyvinyl acetate or Paraloid ™ B-72 was applied. The matrix that encases the fossils at this site is very hard, yet cracks propagate easily. To alleviate cracking from hand tool vibration I employed a gas-powered rock saw. Rock saws caused less vibration that prevented naturally-occurring cracks from opening farther. Air-scribes, pin-vices and the previously mentioned consolidants were employed to prepare Coglan Butte fossils.

Microfossils have been obtained by dry and wet screen sieving of both matrix and anthills. Though most of the rock found at Coglan Buttes resists immediate dissolution,

some beds in the lowest part of the section do break down easily. Over 3,000 pounds of matrix were collected, wet and dry screened and picked for microfossils from UO4166 (Fig. 8). Productive anthills have been collected in localities: UO4183 (Fig. 8), UO4165 (Fig. 9), UO4152 (Fig. 10) and UO4163 (Fig. 11). These were dry screened on site with ¼ inch mesh (visually scanned for bone), and then taken off-site for further processing. Additional treatment included wet screening, drying, and heavy liquid separation. Heavy liquid separation was accomplished using tetrabromoethylene. The specific gravity of the liquid reduced with acetone until a piece of bone from the locality settles out from the lighter minerals and rock fragments. Lighter composition minerals float in slurry while fossil material and heavy minerals settle below. Microfossils and any heavy minerals were then washed with acetone, dried and the concentrated fraction sorted using a stereomicroscope.

All macrofossil measurements reported here were measured with a Whitworth digital caliper, with 0.02 millimeter (mm) accuracy. Fossils smaller than two millimeters were measured by digitally photographing them using a macro lens, including a scale at occlusal surface and measuring in ImageJ (Rasband, 2012).

The taxa described in this paper are represented by the most readily identifiable elements (primarily teeth and tooth-bearing bones) of the fauna. Many described taxa are likely represented in the numerous postcrania found, but these elements are not included unless they were tightly associated with *in situ* cranial material. Of the hundreds of specimens collected thus far, many will require years of work in the future to properly identify to taxon. This is true of most of the hundreds of rodent specimens. Rodents allow tight biostratigraphic interpretation; however, all the rodent specimens (with one

exception) of Coglan Buttes were isolated teeth, none were found in mandibles. These individual teeth will require comparison with more complete dentitions at other institutions. The rodent taxa included in this paper are at least identifiable to genus and will be included to further demonstrate biostratigraphic control. For all teeth discussed in this paper, upper or lower tooth position will be indicated with upper or lower case letters, respectively. Other abbreviations designate position in the toothrow: I/i = incisors, C/c = canines, P/p = premolars, M/m = molars. Abbreviations used in specimen photographs (unless otherwise noted): cm = centimeters, mm = millimeters.

Institutional Abbreviations used in this paper:

AMNH = Department of Vertebrate Paleontology, American Museum of Natural History

F:AM = Frick Collection, Department of Vertebrate Paleontology, American Museum of Natural History

UO = University of Oregon locality

UOMNCH F = University of Oregon Museum of Natural and Cultural History, Fossil (#)

UNSM = Nebraska State Museum, University of Nebraska, Lincoln

USNM = United States National Museum of Natural History, Smithsonian Institution, Washington, D.C.

CHAPTER III

GEOLOGY RESULTS

The lowest geologic unit throughout the study site is andesite. It can be physically traced throughout the study area and an unconformity exists at the contact with the overlying unit. The Guzzler section (Fig. 4) contains the lowest stratigraphic units in the basin. Beardog and Shelter (south to north; Figs. 5-6) are physically correlative laterally, separated by patchy vegetation and soils. Continuous Paisley tuff can be traced from the Guzzler area north through Beardog and Shelter. It also crops out intermittently north of Mylagaulid but is not found at Mylagaulid. In addition, the Paisley tuff can be found in prominent outcrops south of Guzzler.   Mylagaulid (Fig. 7) is approximately 3 kilometers north of Shelter and Beardog sections. Mylagaulid stratigraphy is partially correlative to the Shelter and Beardog sections based on the lithologic similarities of units Ss1, Tp1, Ss2 and Tp2. The pyroclastic flows (Tp1 and Tp2) that cap Ss1 and Ss2 (respectively) are easily recognizable and though they change in thickness across the valley, their lithology and overall internal sequence remains the same. These flows are not physically traceable from Shelter, three kilometers north to the Mylagaulid layer, but their distinctive lithology is unmistakable and offers a basis for correlation.

Volcanic capping rock is physically traceable throughout the entire Coglan Buttes area. It is only directly visible at Mylagaulid, Shelter and Beardog, and thus included in those measured sections. The geology of Mylagaulid, Shelter and Beardog differs significantly from that of Guzzler. The lithology is described briefly in Figs. 8-11 and detailed lithologic descriptions are presented in Table 2.
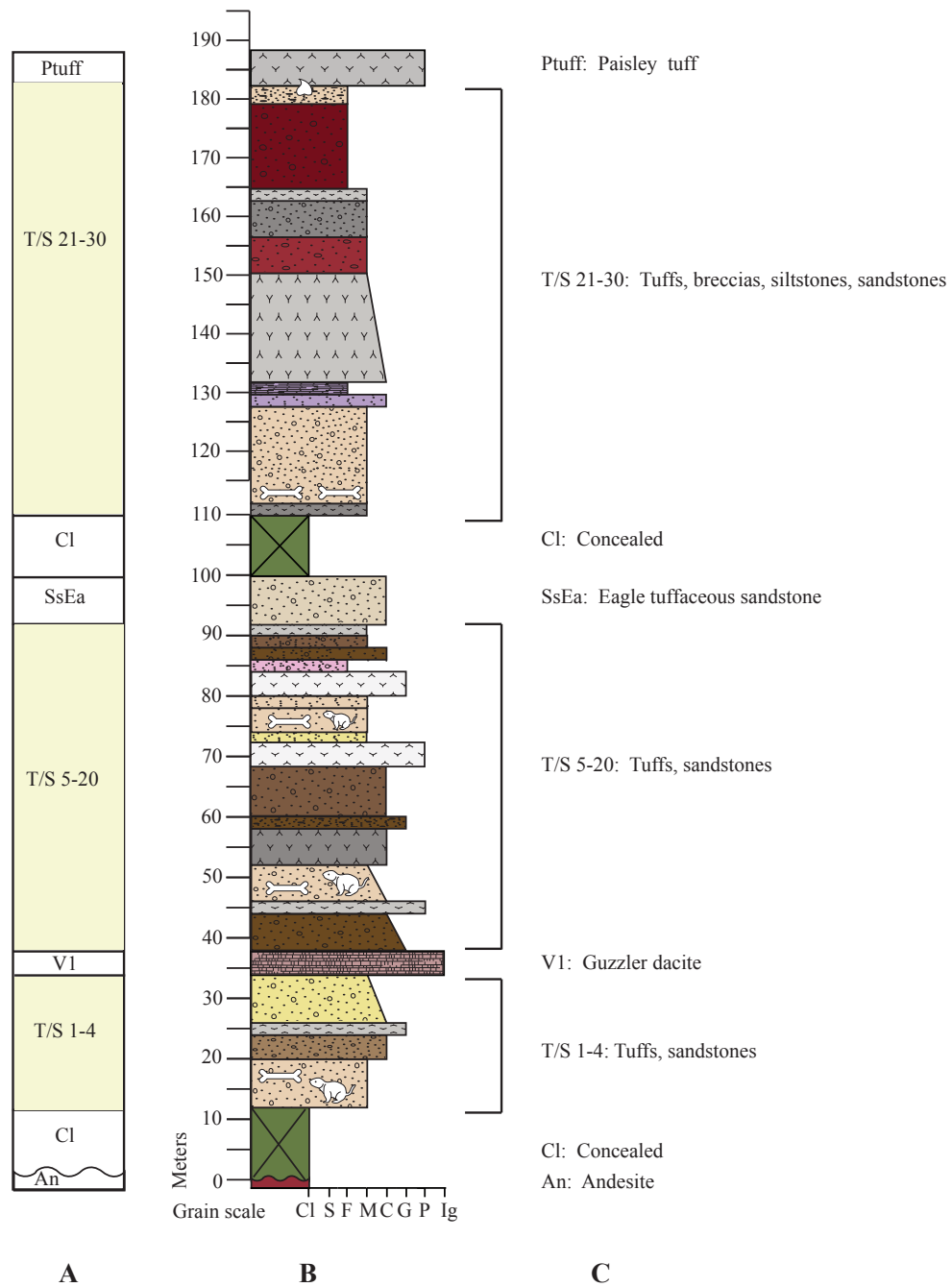
Figure 8. Measured section at the Guzzler area. Collected transects A-A' and B-B' (see Fig 4). (A) Abbreviations for lithologic units and color for corresponding geologic map, (B) stratigraphic section, (C) brief lithology descriptions. Full lithology descriptions are in Table 2. Lithologic patterns are USGS standardized. Grain scale: Cl = Concealed, S = Siltstone, F = Fine sand, M = Medium sand, = Coarse sand, G = Gravel, P = Pebble, Ig = Igneous. Cartoon rodent = microfossils, bone = macrofossils, leaf = plant fossils

17
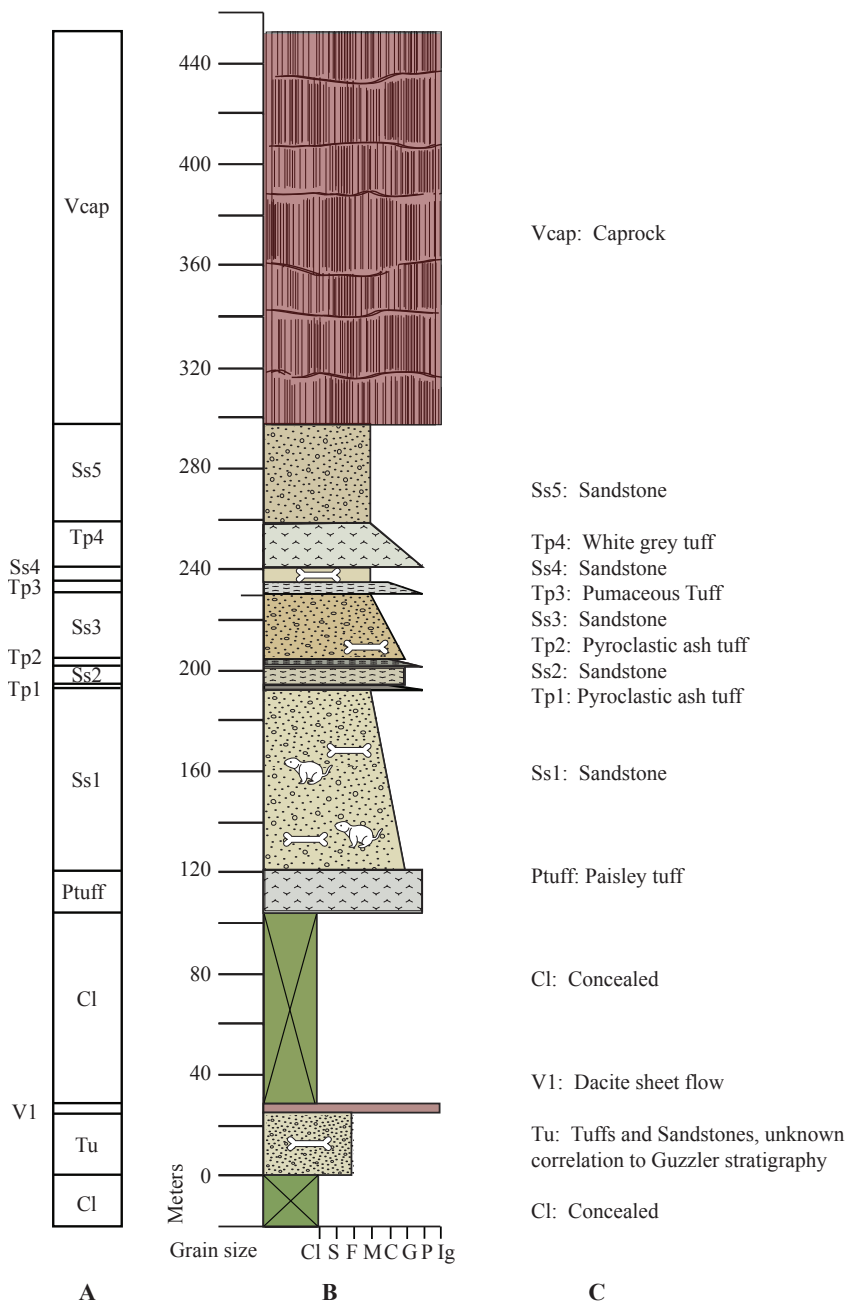
Figure 9. Measured section at the Beardog area. Collected transects C-C' and D-D' (see Fig. 5). (A) Abbreviations for lithologic units and color for corresponding geologic map, (B) stratigraphic section, (C) brief lithology descriptions. Full lithology descriptions are in Table 2. Lithologic patterns are USGS standardized. Grain scale: Cl = Concealed, S = Siltstone, F= Fine sand, M = Medium sand, = Coarse sand, G = Gravel, P = Pebble, Ig = Igneous. Cartoon rodents = microfossils, bones = macrofossils
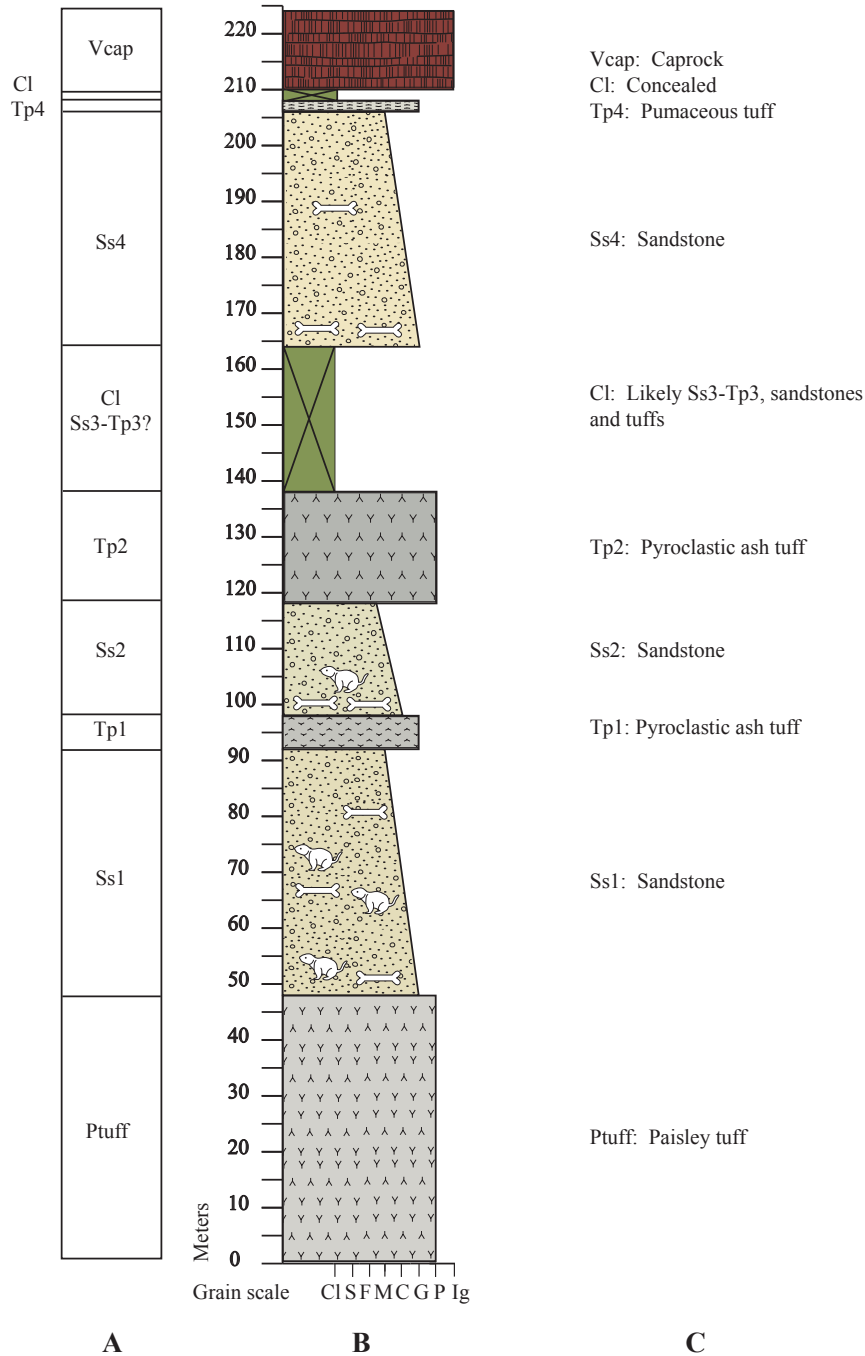
Figure 10. Measured section at the Shelter area. Collected transect E-E' (see Fig. 6). (A) Abbreviations for lithologic units, (B) stratigraphic section (C) brief lithology descriptions. Full lithologic descriptions are in Table 2. Colors and abbreviations are the same for the corresponding geologic map. Lithologic patterns standardized USGS patterns. Grain scale: Cl = Concealed, S = Siltstone, F = Fine sand, M = Medium sand, C = Coarse sand, G = Gravel, P = Pebble, Ig = Igneous. Cartoon rodent = microfossils, bone = macrofossils
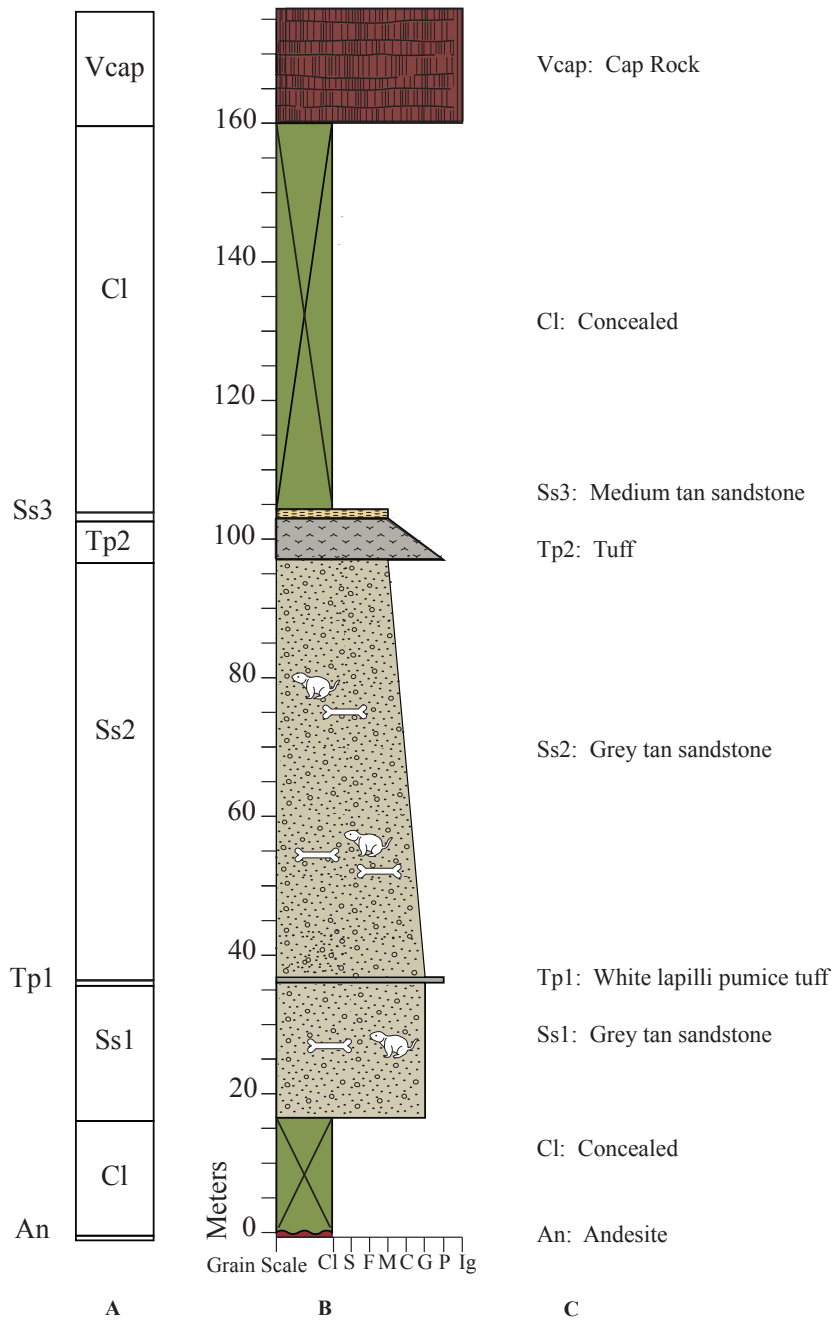
Figure 11. Measured section at the Mylagaulid area. Collected transect F-F' (see Fig. 7). (A) Abbreviations for lithologic units, (B) stratigraphic section, (C) brief lithology descriptions. Full lithologic descriptions are in Table 2. Colors and abbreviations are the same for the corresponding geologic map. Lithologic patterns are USGS standardized. Grain scale: Cl = Concealed, S = Siltstone, F = Fine sand, M = Medium sand, C = Coarse sand, G = Gravel, P = Pebble, Ig = Igneous. Cartoon rodent = microfossils, bone = macrofossils

Table 2. Lithology descriptions. Descriptions and abbreviations for all units found within the sections listed from youngest beds to oldest beds. X = found in that section, - = not found, Cl = concealed.

Sections (North to South)				Abbreviation	Description	Interpretation
Mylagaulid (Figure 11)	Shelter (Figure 10)	Beardog (Figure 9)	Guzzler (Figure 8)			
X	X	X	-	Vcap	Capping unit of entire valley: Flood dacite and basalt sheet flows, generally 3-10 flows visible	Volcanic flows resulting from regional extension
Cl	Cl	X	-	Ss5	Light tan, poorly sorted, tuffaceous medium sandstone, with white pumice lapilli throughout	No discernible bedding or grading of grain size suggest weathering in place of a light debris flow
Cl	X	X	-	Tp4	Pumcaeous, white to gray, unsorted, resistant tuff	Airfall tuff, varies in thickness across sections, indicating moderate paleo-relief
Cl	X	X	-	Ss4	Medium tan-brown, resistant, poorly sorted, fining upward, gravel-course tuffaceous sandstone. Vertebrate macrofossil fragments found in float near bottom contact zone, and *in situ* mandible found at 190 meters in midsection of the unit.	May represent medium energy debris flow, capturing and disarticulating local fauna in the process
Cl	Cl	X	-	Tp3	Massive, fining upward, pebble-coarse, indurated grey-white, pumaceous tuff	Represents an airfall tuff
X	Cl	X	-	Ss3	Thin, medium tan, poorly sorted, coarse sandstone. Vertebrate macrofossil fragments found in float near bottom contact	May represent medium energy debris flow. Vertebrate fossil fragments may be coming from unit Ss4, as no *in situ* specimens have been found in this relatively thin unit. This unit is not observed in Shelter section, but is found in contact with Tp2 in Mylagaulid
X	X	X	-	Tp2	Massive, stratified pyroclastic density current. Alternating ash, lithics, pumice. Some cross- bedding and antidune structures, rip-up clasts, some imbrication and more indurated than the almost identical Tp1	Sustained Plinian eruption, quasi-steady current deposition

Sections (North to South)				Abbreviation	Description	Interpretation
Mylagaulid (Figure 11)	Shelter (Figure 10)	Beardog (Figure 9)	Guzzler (Figure 8)			
X	X	X	-	Ss2	Grayish- tan upward-fining coarse to medium, pumaceous, tuffaceous sandstone. Vertebrate macro- and microfossils found in zones, despite no discernable bedding. *Celtis sp* seeds found ubiquitously throughout. Changes greatly in thickness laterally.	Lateral thickness indicates paleo-relief of low rolling hills, shallow basins. Thickens significantly from south to north. May indicate original massive medium energy debris flow, or fluvial single event deposition.
X	X	X	-	Tp1	Stratified pyroclastic density current. Alternating ash, lithics, pumice. Structures include cross- bedding and antidune structures, rip-up clasts, some imbrication of the larger clasts. Not as massive as Tp2, and much less indurated.	Sustained Plinian eruption, quasi-steady current deposition. Smaller duration eruption than Tp2, though compositionally almost identical
X	X	X	-	Ss1	Grayish tan grading upward into deep brown tan, upward-fining gravel to medium, poorly-sorted, pumaceous, lithic sandstone. Angular cobbles found intermittently throughout. Vertebrate micro- and macrofossils and *Celtis* seeds throughout, but not in the top two meters. Fossils found articulated in zones, though no obvious bedding planes are seen, and disarticulated remains distributed throughout. Thickness varies significantly laterally but composition does not. Top two meters may be an immature paleosol, indicated by marked change in color and burrows in the top half-meter.	Possibly medium to high-energy debris flows or mass wasting events. In the Beardog area, on the southern edge of UO4156 (Fig. 5), there is a 15m wide (by about 10m thick) of very friable, lightly bedded course-pebble pumice lapilli and lithics. This area indicates reworking by a medium energy stream or excess water in the debris flow.

22

Sections (North to South)				Abbreviation	Description	Interpretation
Mylagaulid (Figure 11)	Shelter (Figure 10)	Beardog (Figure 9)	Guzzler (Figure 8)			
Cl	X	X	X	Ptuff	Massive, gray to white, unstratified, lithic, ash tuff flow, with some imbrication and pumice fiamme throughout. Welded and dense near the southern end of Coglan Buttes with subequal lateral thickness. Approximately 0.8 kilometers north of the Guzzler section the bed displays a marked change in density. It is less welded, friable and variable thickness. This unit may be found elsewhere in the Lakeview County.	Massive Plinian eruption, large-scale emplacement of a super heated flow. Where the flow (northern section) is less welded, less dense and expands significantly, emplacement into a body of water or saturated soils is suggested. This northern part of the flow has a sharp contact with the bottom unit, but there is significant load casting, also suggesting emplacement into a saturated soil or body of water. There is no bake zone in this section.
-	-	-	X	T/S 30	Tan siltstone, fossil sedges/grass at contact with Paisley tuff	Very low energy water lain sediments, possibly lake or swamp edge
-	-	-	X	T/S/ 29	Light gray medium sandstone	Low energy fluvial deposition
-	-	-	X	T/S 28	Brick red tuffaceous fine sandstone	Water reworked sediments of underlying unit
-	-	-	X	T/S 27	Dark red, thinly bedded, scoriaceous medium sandstone	Water reworked sediments of underlying unit
-	-	-	X	T/S 26	Dark gray, scoriaceous medium sandstone	Low to medium fluvial deposition
-	-	-	X	T/S 25	Reddish brown bedded tuffaceous medium sandstone	Low to medium fluvial deposition, possibly tuff was airfall
-	-	-	X	T/S 24	Gray tuffaceous coarse to medium, upward-fining sandstone	Fluvial medium deposition, medium to low energy
-	-	-	X	T/S 23	Purple gray foliated sandstone	Very low energy water reworked sediments of underlying unit
-	-	-	X	T/S 22	Purple gray pumice lapilli	Airfall tuff
-	-	-	X	T/S 21	Tan medium tuffaceous sandstone. Vertebrate macrofossil fragments found in float at the contact with the lower unit	Possibly reworked debris flow
	-	-	X	T/S 20	Dark gray sandy tuff	Fluvially reworked tuff
-	-	-	X	Cl	Concealed	Unknown

23

Sections (North to South)				Abbreviation	Description	Interpretation
Mylagaulid (Figure 11)	Shelter (Figure 10)	Beardog (Figure 9)	Guzzler (Figure 8)			
-	-	-	X	SSEa	Tan tuffaceous course sandstone. Named "Eagle", this is unit changes thickness significantly laterally. It is one of the major marker beds of south of the Guzzler section	Debris flow deposition
-	-	-	X	T/S 20	Light gray, medium sandstone	Fluvial deposition
-	-	-	X	T/S 19	Brown, medium sandstone	Fluvial deposition
-	-	-	X	T/S 18	Dark brown scoriaceous medium sandstone	Medium energy fluvial deposition
-	-	-	X	T/S 17	Pink, finely laminated fine sandstone	Very low energy settling sediments
-	-	-	X	T/S 16	Course, white lapilli tuff	Air fall tuff
-	-	-	X	T/S 15	Indurated, tan medium tuffaceous sandstone	Combination airfall tuff and debris flow
-	-	-	X	T/S 14	Tan, medium sandstone. Vertebrate macro- and microfossils (from ant hill) found in float throughout.	Reworked, weathered debris flow
-	-	-	X	T/S 13	Gray brown medium sandstone	Fluvial deposition
-	-	-	X	T/S 12	Yellow pumice lapilli gravel tuff	Airfall tuff
-	-	-	X	T/S 11	White pumice lapilli pebble tuff	Airfall tuff
-	-	-	X	T/S 10	Brown coarse tuffaceous sandstone	Reworked sediment from underlying unit
-	-	-	X	T/S 9	Dark brown scoriaceous gravel	Debris flow, medium energy deposition
-	-	-	X	T/S 8	Dark gray course sandstone	High energy deposition
-	-	-	X	T/S 7	Tan upward-fining coarse to medium sandstone. Locally fossiliferous. Fossils found in float from screening and surface collection. Known as the "*Allomys*" layer after obtaining same from screening.	Debris flow, later weathering and onset of soil formation indicated by rodent fossils present
-	-	-	X	T/S 6	Dark gray gravel-pebble pumice tuff	Airfall tuff
-	-	-	X	T/S 5	Dark brown scoriaceous upward-fining gravel to course sandstone	Possible weathering of under lying dacite sill

Sections (North to South)				Abbreviation	Description	Interpretation
Mylagaulid (Figure 11)	Shelter (Figure 10)	Beardog (Figure 9)	Guzzler (Figure 8)			
-	?V1	-	X	V1	Dacite, named "Guzzler Dacite", may be stratigraphically same as the dacite in Beardog section	Volcanic sheet flows possibly infilling paleovalleys, and these flows are not continuous throughout the southern half of Big Basin
-	-	?T/S 4	X	T/S 4	Yellow, upward-fining gravel to coarse sandstone. In the Beardog, possibly analogous unit vertebrate macrofossils are found in float, though they may be brought down by the large gully from overlying Paisley tuff. In the Guzzler section, this layer produces both and *in situ* and float vertebrate macrofossils.	Debris flow, possible in place weathering in place.
-	-	Cl	X	T/S 3	Grey coarse sandstone with white pumice lapilli throughout	Reworked airfall tuff
-	-	-	X	T/S 2	Light brown coarse sandstone	Fluvial medium to high energy deposition
-	-	-	X	T/S 1	Light tan medium sandstone	Fluvial medium energy deposition
-	-	-	Cl	Cl	Concealed	Unknown
X	-	-	X	Ab	Andesite basement, unconformable contact with upper units.	Andesite rock may be seen, but there is also a zone of andesite cobble observable before being concealed by scree.

Stratigraphic units above the prominent marker bed of the Paisley tuff were originally deposited above the Guzzler section (Fig. 3, in part) but have since been eroded back to the east toward Abert Lake (Fig. 2). Below the Paisley tuff, 33 mostly thinner beds of volcaniclastic airfall tuffs, pumice beds and sandstones record frequent episodes of regional volcanic activity, deposition and subsequent fluvial reworking. The thicker sandstone bed (SSEa; Table 2; Fig. 8) named Eagle tuff is easily traced throughout the southern end of the basin. Eagle tuff, in addition to the prominent ash and pumice layers down section are useful marker beds south of Guzzler. Between Guzzler and Beardog, there is a localized red volcaniclastic bedded dome over which the bedding units down section of the Paisley tuff onlap unconformably and without deformation. This volcanic unit has not been included in the areas of concentrated study and will be investigated in the future. Few of the beds below the Paisley tuff contain fossils. The sandstone units that do produce fossil material mainly contain rodent teeth and macrofauna of relatively small body size.

Although the first few geologic units down section of the Paisley tuff are visible in a few places near the Beardog and Shelter sections, they are not found at the Mylagaulid section. Instead, the Ss1 unit unconformably overlies the andesite unit. The Paisley tuff, although not visible at the Mylagaulid section, does crop out approximately a kilometer to the north and the south (Fig. 3). Notably, all units below the Paisley tuff taper until they thin considerably about 2.5 kilometers south of the Guzzler section (though no sections were measured in this part of the basin).

The Paisley tuff can be traced south of the Guzzler section for approximately eight kilometers. In addition, discontinuous outcrops are found north of Shelter and

approximately five kilometers north of Mylagaulid. South of Guzzler the tuff is

indurated with two apparent zones of cooling. In its southern extent the tuff is uniform in

appearance and approximate thickness. North of Guzzler, in the space of about 10 meters

parallel to strike, the Paisley tuff changes from indurated to friable, however the internal

composition does not change and there is no fault; it is continuous. In addition,

throughout the northern lateral extent, the tuff exhibits eutaxitic texture in the bottom 10-

20 meters of the unit (Fig. 12).
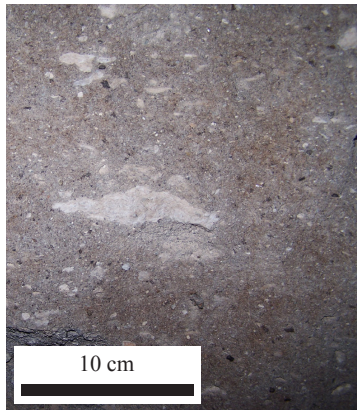
Figure 12. Typical texture of the
Paisley tuff. Eutaxitic texture and
typical pumice fiamme north of
Guzzler.

The contact between the Paisley tuff and the underlying sandstone is significantly

different throughout the northern section versus the southern extent. South of Guzzler the

contact is sharp and there is no deformation of the underlying unit. North of Guzzler, the

contact is again sharp but the weakly-bedded underlying sandstone is deformed. In

addition, irregular load casts of the tuff into the underlying sandstone may are present

(Fig. 13).

27

Figure 13. Typical load cast. Paisley tuff deforming the underlying sediments. Similar structures are found anywhere the contact is visible north of Guzzler.

The units above the Paisley tuff record depositional processes that were very different than those of the Guzzler section. The thick sandstone units do not show bedding except for a ten-meter area in the Beardog section that is moderately bedded. The unsorted, angular grains, ubiquitous large pumice clasts and occasional large, angular cobbles may indicate that these units were debris flows following volcanic eruptions and likely destabilized slopes as a source of sediment (e.g., Huggel, 2008). Partially articulated skeletons are present in zones and could represent capture in the flow. Burrows infilled with finer sandstone are occasionally found in the upper half-meter of Ss1 and Ss2 and permineralized *Celtis* seeds are ubiquitous throughout the beds. This suggests that enough time passed allowing some amount of soil formation.

The pyroclastic density current deposits that cap both Ss1 and Ss2 indicate

Plinean eruptions in the vicinity and exhibit all the internal structure consistent with such

flows (Fig. 14; e.g., Branney and Kokelaar, 2002).

Figure 14. Typical structure of pyroclastic density currents Tp1 and Tp2.

These depositional events appear to have been fairly violent. The basal contacts of Tp1 and Tp2 (where visible) show evidence for disruption of the underlying substrate. Rip-up clasts of the underlying sandstone units are found throughout the outcrops and are incorporated into the bottom layer of the deposit (Fig. 15).

Figure 15. Typical rip-up clasts found at the basal contact with Tp1 and Tp2.

The correlation diagram in Figure 16 illustrates the relationship between the four measured sections. Differences in the thickness of the same units are apparent in the diagram, yet do not capture the variability observed in the field. Between each measured section, bed thickness changes substantially providing evidence for shallow rolling hills and valleys of the paleotopography. The Paisley tuff becomes five times thicker from south to north in the study area. The Ss1 thins from Beardog to Shelter by about half while the Ss2 thickens from Beardog to over six times the thickness at Mylagaulid. Coordinate data for the locations of the measured sections may be found in Table 3.

Table 3. Coordinate data for geologic sections. Starting and ending locations for measured geologic columns from Figs 4-7. Data is in North American Datum 83 (NAD 83), Universal Transverse Mercator (UTM) and uncertainty is 3-9 meters.

Section		Start (Northing, Easting)	End (Northing, Easting)
Guzzler (Fig. 4)	A-A'	4721753, 0718534	4721857, 0718865
	B-B'	4721703, 0718916	4721767, 0719015
Beardog (Fig. 5)	C-C'	4722999, 0718761	4723213, 0719107
	D-D'	4723089, 0719120	4723241, 0719408
Shelter (Fig. 6)	E-E'	4723550, 0718903	4723769, 0719202
Mylagaulid (Fig. 7)	F-F'	4725933, 0715882	4726154, 0716111
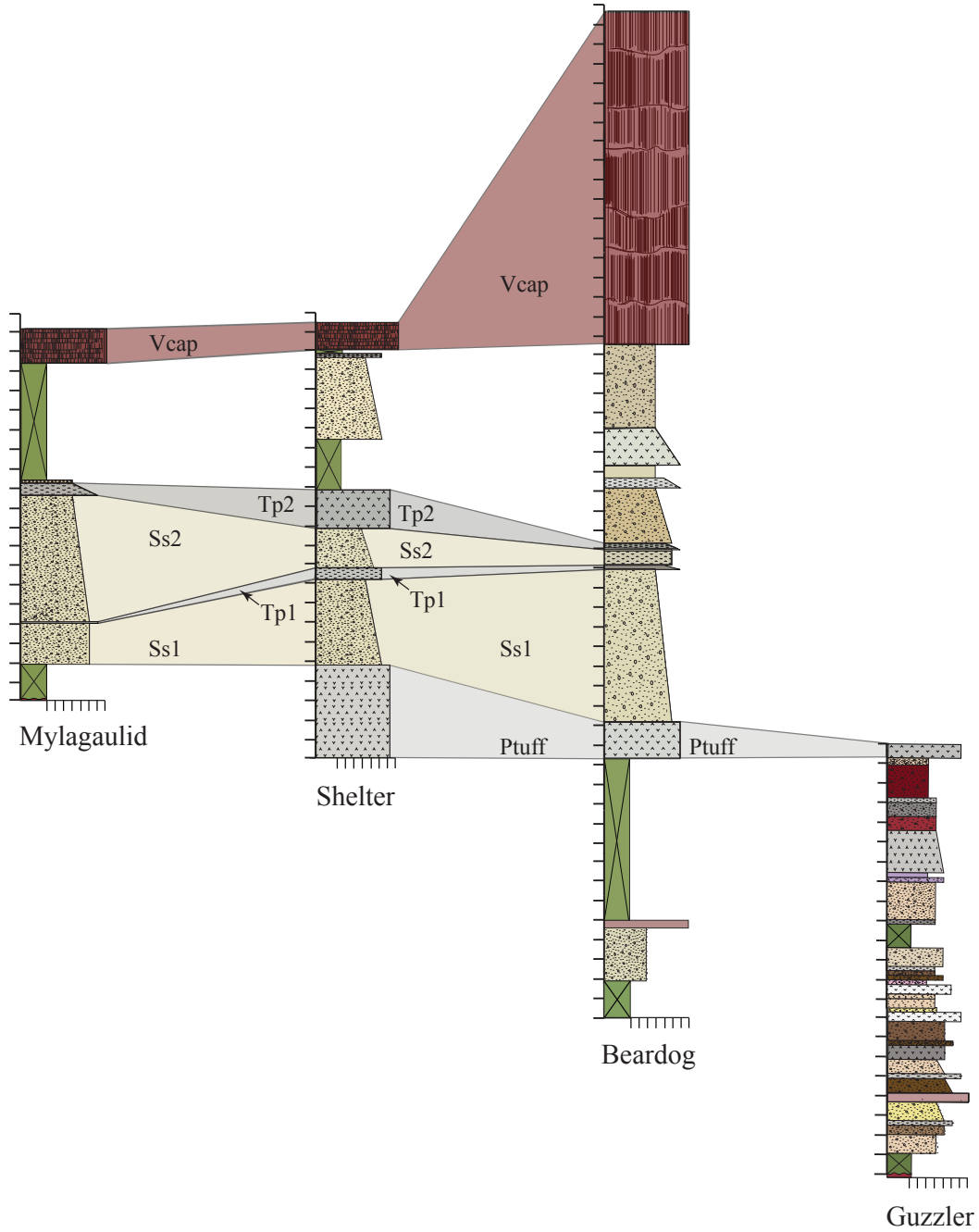
Figure 16. Correlation diagram for the Coglan Buttes stratigraphic sections. Columns scaled down and grain scale preserved from Figs. 8-11. Abbreviations standardized throughout all related figures and defined in Table 2. Tick marks equal 10 meters.

Systematic Paleontology

Class MAMMALIA Linnaeus, 1785

Order RODENTIA Bowdich, 1821

Family MYLAGAULIDAE Cope, 1881

MYLAGAULODON Sinclair, 1903

MYLAGAULODON ANGULATUS Sinclair, 1903

(Figs. 17-18, Table 4)

Referred Material: UOMNCH F-56634, partial skull with I1's, dP3's, P4's, UOMNCH F-56392, left P4; both from UO 4158

Description: UOMNCH F-56634 (Fig. 17) is most of the anterior portion of a skull, forward of the P4's. The left zygomatic arch is flared. The infraorbital canal is deep and recessed into the maxilla. The nasal bones are missing. The frontal bones are very slightly concave. The incisors are strongly curved. The deciduous P3's are very short and peglike. Both P4's have four anteroposterior elongated fossettes; two fossettes are towards the lingual side and two fossettes are towards the labial side. Between the labial fossettes this a smaller rounded fossette on each P4. The P4's are slightly curved; they are concave labially. The mesostyle is prominent on the labial side of the P4, a character lost in most derived mylagaulids.

5 mm

Figure 17. UOMNCH F-56334 ventral view.

32

UOMNCH F-56392 (Fig. 18) is a left P4 and its morphology is essentially identical to UOMNCH F-56334.

Figure 18. UOMNCH F-56392 occlusal view.

Discussion: This species is known from the Arikareean, Kimberly and Rose Creek Members of the John Day Formation (Flynn and Jacobs, 2008; Hunt and Stepleton, 2004). The species is not well known. The genus is based on Sinclair's (1903) description of one specimen, a highly crushed skull with a single P4. The teeth and diastema measurements for Sinclair's (1903) specimen are similar to UOMNCH F-56392 and UOMNCH F-56334 (Table 4). In addition, the four characteristic anterior-posterior fossettes, and the 5th fossette (mesofossette; Korth, 1998), a small lake between the labial fossettes are similar to Sinclair's (1903) description. More common early Miocene mylagaulids, such as *Alphagaulus* and *Hesperogaulus* are more derived; they have anteroposteriorly elongated mesofossettes and additional branching (parafossettes) of the anterior fossette (Korth, 1998; 1999; 2000). The specimens described in this paper represent two individuals and were found approximately 90 meters apart, vertically.

Table 4. Measuements for *Mylagaulodon*. Tooth and diastema dimensions for specimens described in this paper and Sinclair's (1903) *Mylagaulodon angulatus*. APL = anterior-posterior length, TW = transverse width, - = not available. Measurements are in millimeters.

Specimen	I1-P3 diastema	I1 (TW)	P4 (APL)	P4 (TW)
Mylagaulodon angulatus	11.00	2.5	5.50	5.0
UOMNCH F-56334	12.96	2.82	6.72	4.82
UOMNCH F-56392	-	-	6.92	4.62

Order CARNIVORA Bowdich, 1821

Family CANIDAE de Waldheim 1817

(Fig. 19)

Referred Material: UOMNCH F-56383, a right m2 from UO4166

Description: UOMNCH F-56383 (Fig. 19) is subrounded in outline and narrower posterior than anterior. There is a pronounced posterior cingulum, a shallow basin between it and the very worn protoconid. There is a shallow, labial trench between the basin and the protoconid, but not bisecting the posterior cingulum. The anterior root is broken off, and the posterior root is broken vertically.

Discussion: UOMNCH F-56383 was found in the same UO locality as the canid,

Figure 19. UOMNCH F-56383 occlusal view.

Leptocyon (see below). It is morphologically different and significantly larger (length 7.94mm, width 5.66mm) than early canines (Tedford et al., 2009). Its size and morphology are comparable to the hypocarnivorous hesperocyonines and borophagines (Wang, 1994 and Wang et al., 1999).

Subfamily HESPEROCYONINAE Martin 1989

Genus *OSBORNODON* Wang 1994

OSBORNODON IAMONENSIS Sellards 1916

(Figs. 20-25, Tables 5-7)

Referred Material: UOMNCH F-56358 two mandibles of the same individual with partial dentition, partial skeleton from UO4164, UOMNCH F-56379 partial left second premolar, from UO4165, UOMNCH F-56380 right upper second molar from UO4152

Description: F-56358 (Figs. 20, 22) is represented by a right dentary with partial root of c1, anterior root of p2, partial p3, complete p4-m3 (m1 offset by 0.5mm crack), left jaw with partial roots of c1-p4, complete m1 (found in float next to the skeleton), partial root of m2, as well as left and right partial c1's (Fig. 20). The associated postcranial elements were found only centimeters away in the same field jacket; some elements are still articulated and partially encased in matrix. Five partial lumbar vertebrae, three partial caudal vertebrae, complete left calcaneum and astragalus, and many elements of the right pes (Fig. 21) are still articulated.

Figure 20. UOMNCH F-56358 side view. (Top) labial side of right mandible, (bottom) lingual side of left mandible.

Figure 21. UOMNCH F-56358 postcrania. (Left) right calcaneum, (middle) left calcaneum and astragalus, (right) right pes (top is distal and bottom is proximal).

Additional postcrania found in association include the partial distal end of the left femur, a partial proximal fragment of the left humerus, a partial distal right ulna, a partial left distal tibia, a partial left distal radius, the complete right calcaneum, a partial left distal ungual phalanx, the left second phalanx, third proximal phalanx, left navicular, and left proximal metatarsal.

The right dentary is slender and the horizontal ramus is straight with a very slight convex curve on the ventral margin between the talonid basin and ending abruptly at the beginning of the ascending ramus. The ascending ramus is erect, slender, and not shifted laterally. The masseteric fossa is shallow, slightly ovoid, gently tapering anteriorly, and does not invade the horizontal ramus. The angular process is vertically expanded. The angular process cross-section is slightly convexly triangular, and the mandibular foramen is smaller than in other hesperocyonines (Wang, 1994; Fig. 61). The coronoid process is not reduced. The length of the masseteric fossa, depth of condyloid process, height of coronoid process, and depth of horizontal ramus (Wang, 1994) are similar in size to *O. iamonensis*, USNM 8836 (Wang, 1994; Fig. 44). A comparison of *Osbornodon* mandibular measurements compared to UOMNCH F-56358 may be found in Table 5.

Table 5. Measurements for *Osbornodon*. Mandibular measurements after Wang (1994) for *Osbornodon* as available. All measurements in millimeters. LMF-Length of masseteric fossa, HCC[sic]=depth of condyloid process, HCP=Height of coronoid process, DHR=depth of horizontal ramus, n/a = not available

Species	Specimen	LMF	HCC	HCP	DHR
O. iamonensis					
	UOMNCH F-56358	36.39	24.34	53.71	18.72
	USNM 8836	n/a	n/a	55.2	19.66
O. brachypus					
	AMNH 8140	57.4	27.3	59.6	31.4
O. fricki					
	F:AM 27563	56.1	37.5	n/a	37.2
	F:AM 54325	56.8	37.5	75.5	36.6

The right dentition (Figs. 20, 22) includes the partial alveoli of c1, partial root of m1, and partial anterior portion of p3, p4-m3.

Figure 22. UOMNCH F-56358 occlusal view. (Top) right and (bottom) left dentaries.

The p3 occlusal surface is broken, with the exception of the posterior cingular cusp, which is smaller but similar in description to that of p4. The p4 is enlarged, elongate, with a small anterior cingular cusp, a pronounced principal cusp (PC), and a posterior accessory cusp (PAC), and posterior cingular cusp. The posterior cingular cusp (PCC) forms a shallow basin, with small ridges running from the tip of the PCC, mesially tapering and truncates on the buccal side at the notch between formed between PCC and the PAC, and truncates labially at the notch between the principal cusp and the PAC. The m1 is enlarged, with a basined talonid, a pronounced paraconid angled mesially, and a pronounced notch between the paraconid and protoconid. The notch is very wide on the buccal side, narrowing towards and very slightly bisecting the mesial side. The protoconid is separated from the metaconid by a medium notch, angled anterior buccal to posterior mesial. There is a small but distinct buccal entoconid, not separated by a notch. There is a small, enclosed basin between the entoconid and the hypoconid. The talonid is wider than long, and is basined, in contrast to the predominantly trenchant talonids in

most hesperocyonines and borophagines (Wang, 1994, 1999). There is a small, enclosed

basin between the hypoconid and hypoconulid. The posterior border of the talonid is not

convexly angular (as in *Osbornodon brachypus*), but is slightly rounded (Wang, 1994).

The m1 is very worn laterally, with relatively little wear medially. The m2 is elongated,

with a basined talonid, a prominent metaconid, subequal paraconid and protoconid with a

shallow basin in between, and an anterolateral corner cingular cusp. Though Wang

(1994) codes the *O. iamonensis* m2 metaconid character as subequal to the protoconid,

this specimen has much more wear on the lateral edge. The m3 is elongate (2/3 the size

of the m2), shallow, and basined, with subequal paraconid, protoconid, hypoconulid and

hypoconid. This specimen's dental dimensions are on the small end of the range for *O.*

iamonensis (Table 6).

Table 6. Dental measurements for *Osbornodon*. Comparison of UOMNCH F-56358
dental measurements (lowers) to *Osbornodon* species averages reported in Wang (1994;
2003). L= length, W = width, T= trigonid length. All measurements are in millimeters.

		Lp4	Wp4	Lm1	Wm1	Tm1	Lm2	Wm2	Tm2	Lm3	Wm3	Wc1
UOMNCH F-56358												
	Right	10.23	4.91	18.00	7.92	11.9	9.43	6.09	4.96	5.84	3.92	6.52
	Left	-	-	17.01	7.80	11.5	-	-	-	-	-	-
O. fricki												
	Mean	16.61	8.99	27.88	11.69	20.23	12.79	8.23	7.11	7.0	5.88	11.80
	Standard Deviation	0.84	0.53	1.11	0.63	0.97	0.68	0.53	0.56	0.54	0.36	0.68
	Maximum	17.80	9.9	29.7	12.9	21.8	14.1	8.9	8.4	7.80	6.5	13.1
	Minimum	14.9	8.1	26.0	10.6	19.0	11.5	7.4	6.3	6.3	5.6	11.2
	Number	16	15	16	16	16	16	15	14	4	4	5
O. imonensis												
	Mean	11.87	6.32	19.93	8.36	13.58	9.94	6.27	5.47	-	-	6.80
	Standard Deviation	0.51	0.46	1.06	0.37	0.71	0.75	0.39	0.47	-	-	0.00
	Maximum	12.5	7.0	21.5	9.0	14.6	11.5	7.0	6.3	-	-	6.8
	Minimum	10.9	5.4	17.4	7.5	12.3	8.8	5.7	4.8	-	-	6.8
	Number	10	10	11	11	11	10	9	9	-	-	1
O. renjiei												
	Mean	8.30	3.80	12.33	5.75	8.23	6.35	4.40	3.30	3.5	2.70	4.35
	Standard Deviation	0.57	0.25	0.66	0.17	0.38	0.35	0.10	0.10	0.00	0.00	0.35
	Maximum	9.0	4.1	12.9	6.0	8.5	6.7	4.5	3.4	3.50	2.7	4.7
	Minimum	7.6	3.5	11.4	5.6	7.7	6.0	4.3	3.2	3.50	2.7	4.0

		Lp4	Wp4	Lm1	Wm1	Tm1	Lm2	Wm2	Tm2	Lm3	Wm3	Wc1
	Number	4	4	3	4	3	2	2	2	1	1	2
O. scitulus												
	Mean	10.51	5.8	17.76	7.95	12.47	8.65	6.03	4.92	-	-	6.7
	Standard Deviation	0.50	0.61	0.80	0.47	0.74	0.47	0.43	0.56	-	-	0.00
	Maximum	10.9	6.5	18.8	8.5	12.9	9.2	6.6	5.4	-	-	6.7
	Minimum	9.5	4.2	16.6	6.9	10.7	8.1	5.7	4.2	-	-	6.7
	Number	9	10	9	9	9	6	6	6	-	-	1
O. sesnoni												
	Mean	10.05	4.70	14.97	5.75	10.13	8.20	4.85	4.50	4.70	4.00	-
	Standard Deviation	0.25	0.28	0.34	0.17	0.24	0.10	0.05	0.00	0.00	0.00	-
	Maximum	10.3	5.1	15.3	6.0	10.3	8.3	4.9	4.5	4.70	4.00	-
	Minimum	9.8	4.5	14.5	5.6	9.8	8.1	4.8	4.5	4.70	4.00	-
	Number	2	3	3	4	3	2	2	1	1	1	-

The partial anterior portion of the left ramus is too fragmentary to obtain comparable measurements, however, it is a mirror of the right side. The left dentition is mostly absent. The partial c1 is slender with a weak posterior ridge and the base of what may have been a more pronounced anteromedial ridge. There are roots of p1, p2, anterior root of p3, and anterior root of p4. The m1 was found in float, directly adjacent to the *in situ* skeleton. It is a mirror image of the right m1, with identical wear pattern, and identical morphology. It is safe to assume that it is from the same individual.

Postcrania measurements of *O. iamonensis* have not been published. The measurements of this specimen's postcranial dimensions follow Wang's (1993) treatment of an early canid, *Hesperocyon* and Munthe's (1989) study of borophagine postcrania.

Table 7. UOMNCH F-56358 postcrania measurements. Measurements after Munthe (1998; Fig. 2). All measurements in millimeters.

Tibia distal width	20.45
Ulna distal width	12.31
Radius distal width	21.24
Right calcaneum length	35.97
Right calcaneum tuber length	25.29
Left calcaneum length	35.45
Left astragalus length	21.94
Left astragalus trochlea width	11.50

There is 121millimeters (mm) preserved of the distal right ulna (Fig. 23). It is not robust, as in more primitive canids (Wang, 1993) and about the same thickness as the distal portion of the radius. The styloid process is sub-rounded, and not reduced. The interosseous crest is pronounced, bordered by fairly deep grooves. The distal portion of the radius (Fig. 23) has a sharply pronounced but reduced styloid process. The anterior surface has a prominent process separating two deep grooves. There is 122mm left tibia preserved (Fig. 23) it is missing most of the proximal quarter of the shaft, and is crushed proximally, but relative complete distally. The medial malleolus is pronounced, slightly rounded and comes to a gentle rounded point posteriorly. The lateral malleolus is pronounced, but shorter than the medial, and the dorsal projection is only slightly shorter than the lateral. These processes form a deep trochlea. The articular surface of the left astragalus is obscured; it is articulated with the calcaneum (Fig. 21). The tuber is reduced, shifted medially, and without a lip. The trochlea is moderately sharp, in proportion to the distal tibia trochlea, and does not have any processes that would inhibit full range of the tibia over the trochlea. There is no tubercle on the proximal end of the medial trochlear rim. The calcanea are slender, with a pronounced groove on the distal, ventral side. The medial articular surface is adjacent to the lateral articular surface.

Figure 23. UOMNCH F-56383 limb bones. (Left) left distal tibia, (middle) right distal ulna, (right) left distal radius.

UOMNCH F-56379 (Fig. 24) is the labial half of a left p2 (broken dorsal ventrally), but still has most of its two roots and principal cusp.

Figure 24. UOMNCH F-56379 labial view.

The anterior cingular cusp and posterior accessory cusp are subequal and closely appressed to the principle cusp. There is a very small posterior cingular cusp, slightly expanded caudally, though not nearly as much as the p3-4 of UOMNCH F-56358. Specimen UOMNCH F-56380, a right upper second molar (Fig. 25) has a subequal paracone and metacone, broad internal cingulum, and a shallow basin between the

preprotocrista and internal cingulum. The M2 is enlarged (relative to other hesperocyonines and borophagines) and ovate, as is characteristic of *Osbornodon iamonensis* (Wang, 1994).

Figure 25. UOMNCH F-56380 occlusal view.

Discussion: The stratigraphic unit where UOMNCH F-56358, F-56379 and F-56380 were found contains other Late Arikareean taxa. These three specimens were found in the same Ss1 stratigraphic unit, mid-section (Figures 9-11, Table 2) though in localities (UO4164, UO4165, UO4152) laterally separated by several hundred meters. Six borophagines and two hesperocyonines could potentially occur coevally during this geologic time frame. The left and right m1 of UOMNCH F-56358 lack protostylids diagnostic in borophagines (Wang et al., 1999). Most hesperocyonines were hypercarnivorous and had a reduced p2 and m2, and a trenchant m1 talonid (Wang, 1994). However, the hesperocyonine genus *Osbornodon* was hypocarnivorous, with basined m1s, talonids that were wider than long, elongated m2s and expanded, enlarged m1-2 (Wang, 1994), as seen in UOMNCH F-56358 and UOMNCH F-56380. Within the *Osbornodon* clade, two candidates, *Osbornodon renjiei*, *Osbornodon sesnoni*, may be ruled out, in part, because they are not known to occur in the Arikareean (but much earlier in the Whitneyan)(Wang, 1994; 2003). More significantly all tooth dimensions of UOMNCH F-56358 far exceed those of *O. renjiei* and *O. sesnoni* (Table 6).

43

Of the remaining options within the *Osbornodon* clade (*O. iamonensis*,

Osbornodon brachypus, *Osbornodon fricki*, and *Osbornodon scitulus*), some are easily

dismissed, but the latter requires substantial discussion. Though Wang (1994) does not

report tooth dimensions for *O. brachypus*, (a late Arikareean species), it is distinct from

O. iamonensis in that it has substantial diastema between all premolars, and a convex,

posteriorly-pointed talonid (Wang, 1994); characters not observed in UOMNCH F-

56358. Additionally, *O. brachypus* does not have anterior cingular cusp or posterior

cingular cusp on the p2-3, unlike UOMNCH F-56379. The M2 is more problematic to

exclude from *O. brachypus,* as Wang (1994) describes its shape and morphology as

similar to *O. iamonensis,* yet of much smaller dimensions. Without further figures or

dimensions in the literature to compare, absolute diagnosis may be impossible. It seems

more likely, however, that UOMNCH F-56380 would be *O. iamonensis* given its

occurrence in the same horizon and locality as other specimens definitively referable to

O. iamonensis.

O. *fricki*, a middle Hemingfordian species, has substantially larger tooth

dimensions than *O. iamonensis*, its posterior mandibular features do not resemble *O.*

iamonensis (Wang, 1994; Fig.61). *O. iamonensis'* mandibular foramen is much smaller

and not as incised, while *O. fricki'*s is larger diameter and more deeply incised. *O.*

iamonensis' coronoid process is more erect than the flatter, less robust one of *O. fricki*.

The angular process of *O. iamonensis* is sharply pointed posteriorly with a dorsally

concave triangular cross section while that of *O. fricki* is rounded in cross section and

more blunt posteriorly. The paracone is much greater than the metacone on the M2 of *O.*

fricki, unlike UOMNCH F-56380. The size and morphology of an *O. fricki* p2 is

reduced, with a significantly reduced, very low posterior cingulum, not pronounced and posteriorly expanded as in UOMNCH F-56379. UOMNCH F-56358, F-56379 and F-56380 are not referable to *O. fricki*.

Though Wang (1994) discusses the Hesperocyninae exhaustively, material discovered much later allowed Wang (2003) to re-evaluate both *O. scitulus* and *O. iamonensis*, as both species were rather vaguely defined in the literature, and often confused for one another. The tooth dimensions of UOMNCH F-56358 more favorably compares to those of *O. scitulus* (Table 6). However, they are not outside of the minimum tooth dimensions for *O. iamonensis* (Wang, 1994). Wang (2003) considered *O. scitulus* to be more derived than *O. renjiei* and *O. sesnoni*, but more primitive than *O. iamonensis, O. brachypus,* and *O. fricki.   O. iamonensis* can be distinguished from *O. scitulus* by a less robust jaw, a distinct anterior accessory cusp on the p4, an entoconid smaller than hypoconid on the m1, and a longer m2 with a relatively strong anterior cingulum (Wang, 2003). Additionally, in *O. scitulus* the M2 metastyle is reduced to a tiny postprotocrista, and the p2 is reduced to a single main cusp, both of which are not found in of UOMNCH F-56358 and F-56380. UOMNCH F-56358 also exhibits all of the features considered to distinguish *O. iamonensis* from *O. scitulus.* Although UOMNCH F-56358 is nearest the minimum tooth dimension for *O. iamonensis*, and compares more favorably to *O. scitulus* tooth dimensions, it clearly exhibits tooth morphology consistent with *O. iamonensis*.

It is interesting to note that the highest diversity of the carnivore guild was in the early Arikareean, and competition for meat sources may have driven early hesperocyonines to radiate into omnivorous roles (Van Valkenburg, 1991). UOMNCH F-

56358, F-56379 and F-56380 were found in the same stratigraphic layer with a more hypercarnivorous canid, *Paracynarctus* (UOMNCH F-56317), evidence of sympatry and for some degree of niche partitioning within the carnivorous fauna of Coglan Buttes. These two canid species found in Ss1 are not found in the John Day Basin (Albright et al. 2008).

Postcrania of *O. iamonensis* have not previously been described in the literature. However some conclusions may be drawn from the associated postcrania of UOMNCH F-56358, in light of Wang's (1993) work on *Hesperocyon* postcrania discussing canid functional morphology. *Hesperocyon*, the most primitive canid from the late Eocene to early Oligocene) was plantigrade, probably scansorial, yet had full rotation of the tibia through the astragulus (Wang, 1993). Later and morphologically more derived *Osbornodon* share a few primitive characteristics of the basal canids, yet had a more dedicated partial digitigrade stance, though not as cursorial as later canines (Wang, 1993). Cursorial animals tend to reduce the thickness of the distal ulna shaft relative to the distal radius (Wang, 1993). The distal radius and ulna of UOMNCH F-56358 are subequal in diameter and not thin and tapering as in cursorial canids (Wang, 1993). The styloid process of the ulna is subrounded, and not reduced as in more primitive Hesperocyonines, but not as pronounced in later more derived canines (Wang, 1993). Furthermore, the radius of UOMNCH F-56358 still possesses the primitive trait of a prominent process on the anterior side. This character is retained in more primitive canids such as *Hesperocyon*, but lost in more derived canids, and virtually lost in modern canids (Wang, 1993).

The astragalus and calcaneum of UOMNCH F-56358 exhibit characters of a digitigrade stance. There is no tubercle on the proximal end of the medial trochlear rim of the astragalus, which is found in plantigrade carnivores (Wang, 1993). The medial articular surface of the calcaneum is adjacent to the lateral articular surface, and is considered an advanced character in canids (Wang, 1993). UOMNCH F-56358, an *Osbornodon iamonensis*, was likely fully digitigrade, yet not fully cursorial.

Subfamily BOROPHAGINAE Simpson, 1945

Subtribe CYNARCTINA McGrew, 1937

Genus *PARACYNARCTUS* Sp. Wang 1999

(Fig. 26)

Referred Material: UOMNCH F-56317, right mandible, alveoli of i3, c1, p1, partial p2, alveolus p3, partial p4, partial m1, alveoli of m2 and m3, from UO 4156.

Description: The horizontal ramus (Fig. 26) is slender both in length and width and slightly tapers anteriorly.
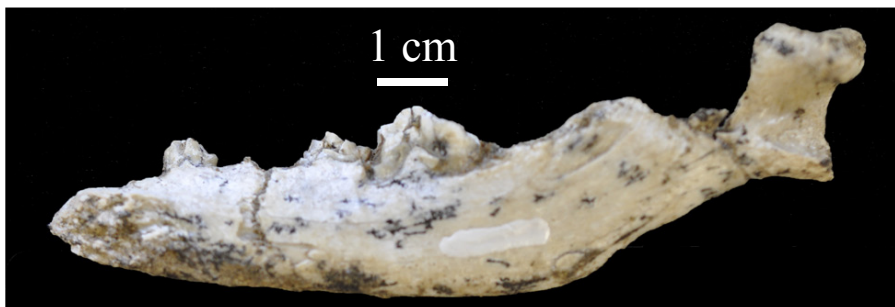

Figure 26. UOMNCH F-56317 lingual view.

There is a convex subangular lobe on the ventral posterior horizontal ramus, the apex of which is vertical to the posterior m2 root. The masseteric fossa is deeply excavated and

tapers anteriorly without a pocket. The ascending ramus is missing. The angular process is broken, but enough remains to see that it initially angles ventrally and in cross-section is subangular, concave and (labially) V-shaped. The condyle is neither erect nor diminished and is higher than the tooth row. The condyle shows signs of postmortem gnawing by rodents, as does most of the ascending ramus; there are parallel grooves, less than a millimeter wide all along, likely from a rodent pre-burial. There are alveoli for the i3, c1 and p1. The double rooted p2 is partially broken on the anterior lingual side. The anterior cingular cusp is very reduced labially and partially broken lingually. The principal cusp is low and not very angular. There is no posterior accessory cusp and the posterior cingular cusp is very reduced to only a slight shelf with a slight high point oriented posteriolabially. The double-rooted p3 is missing. The p4 is broken lengthwise lingually, but the anterior cingular cusp is more pronounced. The principal and posterior accessory cusps are broken but the bases indicate they were moderately robust, yet low. The posterior cingular cusp is substantial and is wider than the width of the principal cusp; it has a small ridge that runs labially to the base of the principal cusp. There are very slight diastemata between the premolars. The m1 trigonid is mostly broken off lingually. The talonid is heavily worn lingually and with a small notch broken medial posteriorly, but the width is narrower than the trigonid. The m2 is double-rooted and the m3 has a single root angled upwards towards the ascending ramus.

Discussion: Though the m1 (highly diagnostic for carnivores) is broken and very worn, UOMNCH F-56317 retains many characters that allow its diagnosis as *Paracynarctus* sp. Most borophagines have a slightly rounded, ventrally convex, deep, robust horizontal ramus with the exception of *Cyanartoides, Paracynartus* and *Cynarctus* (Wang et al.,

1999). These genera have a more shallow, slender rami with a distinct subangular lobe near the posterior and a condyle that is elevated above the tooth row (Wang et al., 1999), as does UOMNCH F-56317. Wang (1994) considered the posterior morphology, especially the angular process of the ramus to be significant in the diagnosis of hesperocyonines. The angular process cross section of UOMNCH F-56317 does resemble that of *Osbornodon*, but shares no other ramus characteristics with that genus or any of the hesperocyonines (Wang, 1994).

All tooth dimensions of UOMNCH F-56317 far exceed (by more than 2x) any known Arikareean or early Hemingfordian canine (Tedford et al., 2009). Additionally, UOMNCH F-56317 premolars retain the posterior accessory cusp and posterior cingular cusp. They are not reduced in morphology, nor have high, pointed, vertical principal cusps as in canids (Tedford et al., 2009) and amphicyonids (Hunt, 2011).

Of the eligible borophagine candidates, UOMNCH F-56317 tooth dimensions are double those of all the possible species of *Cynarctoides* (Wang et al., 1999). UOMNCH F-56317 shows tooth dimensions that are more similar to *Paracynartus* and *Cynarctus*, however the latter is first known from the early Barstovian (mid-Miocene) (Wang et al., 1999). Though *Paracynartus* is only known to have first appeared in the earliest Hemingfordian (Wang et al., 1999), the Ss1 unit (Figures 5-7) produces many taxa indicative of a late Arikareean age. In addition, Wang et al. (1999; Fig. 141) suggest the predecessor for *Paracynartus* and the rest of the cynarctines should be found in the latest Arikareean. UOMNCH F-56317 may indicate a range extension for the species, though better material with a fully preserved m1 would be necessary before a definite first appearance can be established.

Subfamily CANINAE Fischer de Waldheim, 1817

Subfamily CANIDAE Fischer de Waldheim, 1817

Genus *LEPTOCYON* Sp. Matthew, 1918

(Fig. 27, Table 8)

Referred Material: UOMNCH F-56381 partial right edentulous anterior mandible,

alveoli and partial roots of c1-anterior root of p4, from locality UO4166

Description: This partial mandible (Fig. 27) is slender and shallow with a maximum

depth of 6.8 mm at the p4 alveolus. It tapers slightly towards the c1.

The minimum dimensions for the missing teeth are found in Table 8 and were obtained

by measuring to the outside edge of the alveoli. There is a small posterior mental

foramen beneath the slight diastema between the p2 and p3. An anterior mental foramen

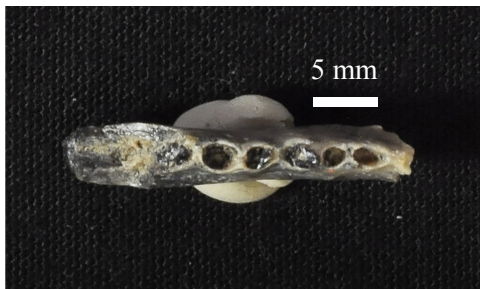is beneath the anterior p2 root.

.

Figure 27. UOMNCH F-56381
occlusal view.

Table 8. Measurements for UOMNCH F-56381. Minimum values for missing teeth in
UOMNCH F-56381, - = not available, measurements are in millimeters.

UOMNCH F-56381	p1	p2	p3	p4
Length	2.75	4.76	5.88	-
Width	1.62	1.76	2.39	2.5

Discussion: The overall small, thin, shallow ramus size and linear arrangement of a full complement of premolar alveoli of this specimen excludes is from all carnivores except the canids. Canids of this size are restricted to the genus *Leptocyon*, a genus that is found in earliest Oligocene to the late Miocene (Tedford et al., 2009). The minimum measurements of UOMNCH F-56381 fall well within the range of early to medial Arikareean *Leptocyon* and are smaller than all younger species, except one species found in the Hemingfordian through Barstovian (Tedford et al., 2009). Of note, UOMNCH F-56381 is smaller than the minimum tooth dimensions for *L. vulpinus*, found exclusively in the medial Arikareean through the early Hemingfordian (Tedford et al., 2009). It is likely that UOMNCH F-56381 represents an Arikareean species.

Family CAMELIDAE Gray, 1821

Subfamily FLORATRAGULINAE Maglio, 1966

Genus *AGUASCALIENTIA* Sp. Stevens, 1977

(Figs. 28-30, Table 9)

Referred Material: UOMNCH F-56342 partial right cranium with P4 and M1-3 and most elements from the limbs, from UO 4158, UOMNCH F-56352, a partial left mandible with m2 and anterior portion of m1, from UO 4162, UOMNCH F-56354, the anterior fused partial mandible with root of right p1, c1, i1-3 and left i3, c1, p1 and partial alveoli of p2, from UO 4158. All referred material was found *in situ*.

Description: UOMNCH F-56342 (Fig. 28) is most of the right side of a cranium.
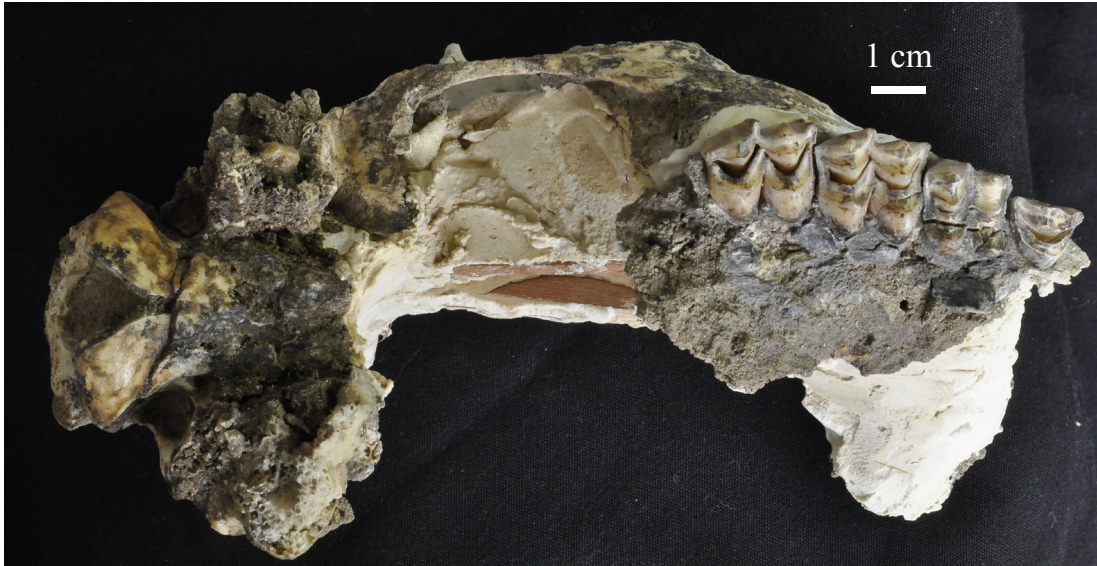
Figure 28. UOMNCH F-56342 ventral view.

The right bulla is mostly missing but the left bulla is noticeably large for a camelid. It is 44.80 mm at its longest tranverse dimension. In its eroded state, it is dimensionally larger than the complete occipital condyle. The zygomatic arch is noticeably delicate and thin for a camelid and encloses the orbital foramen. The brain case is short and rounded. The sagittal crest is small but raised to a sharp edge. The lambdoidal crest does not flare past the edges of the occipital condyle. The P4 has a strong lingual lobe, a completely enclosed deep rounded U-shaped fossette, strong parastyle and strong metastyle. The M1 is anterior posteriorly compressed, bi-lobed with a strong mesostyle and metastyle, a posterior lobe that is slightly larger than the anterior lobe. There is a worn but visible labial inter-columnar tubercle between the lobes. The M2 and M3 are very similar to the M1; both have very strong parastyles, mesostyles and weaker metastyles. Both have strong labial ribs that terminate at the paracone and metacone. Both posterior lobes are wider than the anterior lobes, but the M3 posterior lobe is transversely narrower than the anterior lobe. The M2's intercolumnar tubercle is more prominent than in the other

52

molars. In addition, it has a strong cingulum on the anterior side and a weaker cingulum on the posterior side. The M3 intercolumnar tubercle is strong, but not as large as in the M2. Both M2 and M3 have deep fully enclosed V-shaped fossettes. The M3 cingula are similar to the M2. All teeth are brachyodont.
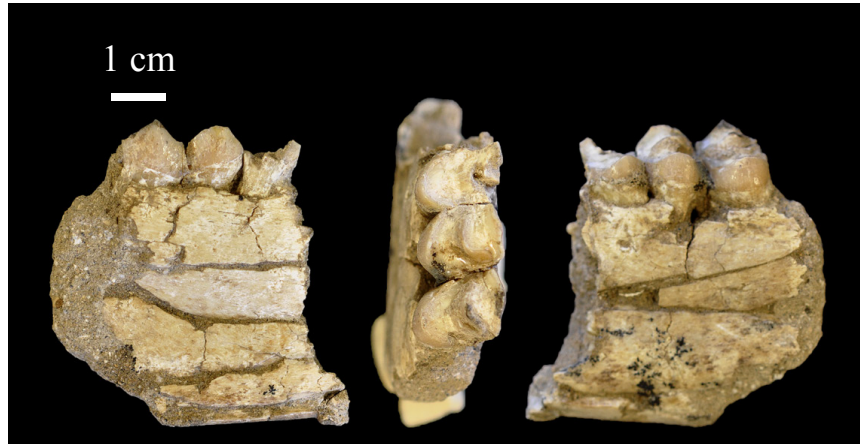
Figure 29. UOMNCH F-56352 three views. (Left) lingual view, (middle) occlusal view, (right) labial view.

UOMNCH F-56352 (Fig. 29) is a fragment of a left mandible. The mandible is shallow and thin with brachydont molars. The m2 is entire, with strong, high metaconid and entoconid coming to sharp points, strong labial lobes. The anterior fossette is pinched almost shut near the posterior end and very shallow on the anterior end. The posterior fossette is not an open dentine V, but forms a dentine open loop on its anterior end, and is only a dentine edge on its posterior end. The M1 anterior lobed is worn past its fossette depth.

UOMNCH F-56354 (Fig. 30) is the anterior portion of fused mandibles. The horizontal ramus posterior to the p1 tapers posteriorly and thins. The symphysis is deep

and robust. The fused portion of the mandibles angles dorsally beginning at the posterior towards the anterior.
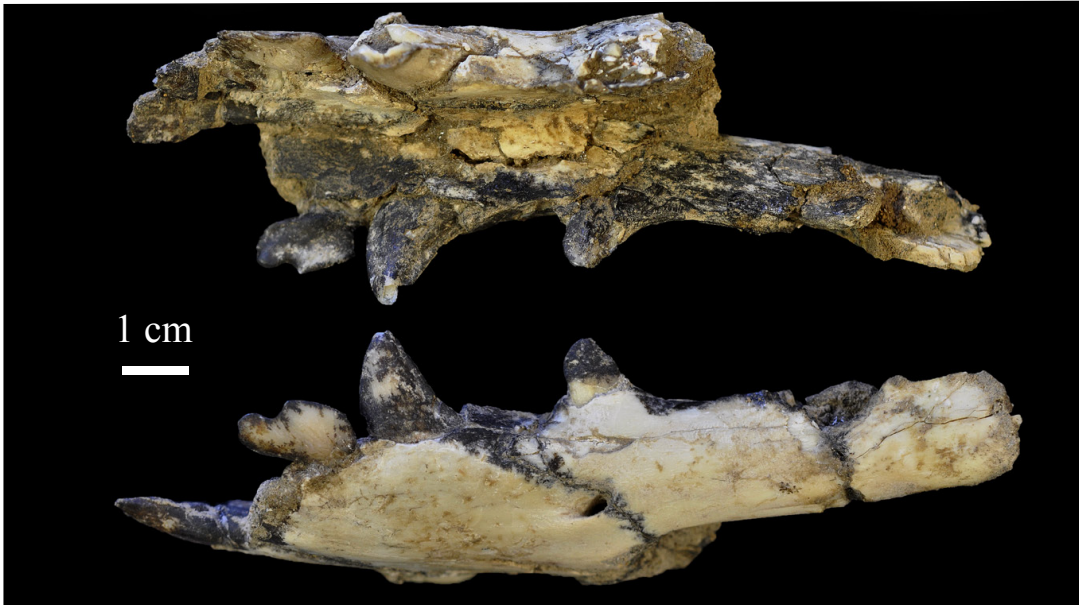
Figure 30. UOMNCH F-56354. (Top) dorsal view, (bottom) side view.

The terminus of the ramous is rounded, allowing sufficient room for the incisors. The lingual surface of the symphysis is trough shaped, shallow anterior but deepens towards the posterior. All incisors have net-like plications on the buccal surfaces. The right i1 is elongate, spatulate on the occlusal surface, and tapers from the medial edge laterally with a notch on the right medial edge. The i2 is broken but the remaining shape indicates it was similar to i1, only slightly enlarged. Both i3's are positioned laterally and are more strongly spatulate, with a deeper notch on the occlusal surface than i1 and i2. All incisors are expanded, robust, and though overlapping they are not crowded. Both canines are robust, short, with strong sharp edges anterior and posterior, oval in cross section, recurved with deep robust roots. There is a short diastema (right side 18.34 mm, left

15.42 mm). The difference in diastema appears to be postmortem crushing.   The left

sub-caniniform p1 has a single robust root and is shorter than the canine. The mandibular

foramen is deep and pocketed, with the opening oriented posterodorsally. UOMNCH F-

56354 was found with UOMNCH F-56355 (unfused articulated distal metapodials)

several centimeters away. They are likely from a juvenile, as the epiphyses are missing.

The posterior sides have slight grooves that deepen proximally.

Discussion: UOMNCH F-56342 differs from all stenomylines and basal camelids in that

it does not have high-crowned teeth with reduced parastyles, mesostyles or metastyles

nor a reduced P4 (Honey et al., 1998). Specimen UOMNCH F-4158 is excluded from

basal camelids such as *Poebrotherium* and stenomylines because the incisors are not

reduced (Honey et al., 1998). The canines of UOMNCH F-56354 are not incisiform and

the lower molars of UOMNCH F-56354 are lobed and low-crowned (Honey et al., 1998)

thus excluding them from the stenomylines or basal camelids (Frick and Taylor 1968 and

Honey et al., 1998). Miolabines have a caniform I3, p1 normally absent or double rooted,

hypsodont molars without labial ribs, all molars with reduced morphology relative to

other camelids (Honey et al., 1998). Thus all referred specimens discussed here are

excluded from the subfamily Miolabinae.   Additionally, these specimens are excluded

from the protolabines for lack of a caniform I3, unreduced c1 and molar lobes subequal

instead of unequal (Honey and Taylor, 1998). Exclusion from the remaining Camelidae

is more problematic. The name, Camelidae is used as a "garbage taxon", and includes

many genera (namely *Oxydactylus)*, which have many but not all characters similar to the

specimens discussed here (Matthew and MacDonald, 1960).

55

UOMNCH F-56342 is assigned to *Aguascalientia* based on its molar morphology but mainly its strong cingula on the anterior and posterior molars and the very strong intercolumnar tubercles on all molars, characters found on most floridatragulines and all *Aguascalienta* (Honey et al., 1998; Stevens, 1977; Rincon et al., 2012). Its unusually large bulla and intercolumnar tubercles are characters shared with the floridatraguline *?Poebrotherium franki* (Honey et al., 1998; Rincon et al. 2012). The very delicate zygomatic arch is inconsistent with any known camelid description. *Aguascalienta* has been found previously in the Early Late Arikareean-Early Hemingfordian of the Delaho Formation of southern Texas, and the Late Arikareean-Late Hemingfordian of an unnamed formation in northern Mexico. Its sister floridatragulines have been found in Texas, Florida, and northern Mexico. UOMNCH F-56342 may well be a new species of the genus.

UOMNCH F-56354's "leaf-like" (Honey et al., 1998) incisors represent a character shared with ?*Poebrotherium franki* and most of the floridatragulines to some degree, yet its symphysis does not begin under the p2, but under the p1 and is a character shared with *A. panamaensis*. As well, the distinctly short oval strongly caniniform canine are characters used to describe *Aguascalientia* (Honey et al., 1998; Rincon et al., 2012), but *A. panamaensis* has a much smaller c1 than in this specimen. At best, UOMNCH F-56354 can be assigned to the genus *Aguascalientia*. Of note, it was found *in situ* just two meters lateral and about a quarter meter (m) below from UOMNCH F-56342 in a small (~10 m x 20 m) outcrop that also produced other camelid skeletal parts (not yet prepared or described). It may represent a small death assemblage of part of a herd. The unfused metapodials, UOMNCH F-56355, found centimeters away from UOMNCH F-56342 may

or may not belong to the same individual. The tentatively assigned *Aguascalientia* distal metapodials of Stevens (1977) show them as unfused but that is true of most Arikareean and early Hemingfordian camelids (Honey et al., 1998). The metapodials found associated with UOMNCH F-56355 though likely *Aguascalientia* given all fossils from the immediate vicinity are also *Aguascalientia*, cannot be definitively assigned to the genus.

UOMNCH F-56352 is assigned to *Aguascalientia* based on its closed loop of dentine on the anterior fossette of m2; it is a unique character that has only been described in *A. panamaensis* and no other camelid (Rincon et al., 2012). Additionally, its molar morphology is consistent with *Aguascalientia*, though many of the floridatragulines have similar lower molar description (Stevens, 1977; Honey et al., 1998). The dimensions of UOMNCH F-56352 molars do exceed those of *A. panamaensis* (Table 9). The uniqueness of the dentine loop, yet dissimilar size, and the previously discussed specimens further support the possibility that these specimens represent a new species of *Aguascalientia*. UOMNCH F-56352 was found in the same Ss2 unit (UO 4162; Fig. 11) that the previously discussed specimens were found, though a little over 800 feet to the southeast. Tooth dimensions for all specimens referred to *Aguascalientia* in this paper are compared with those available from Rincon et al. (Table 1; 2012) in Table 9.

Table 9. Dental measurements for *Aguascalientia* sp. Comparisons of tooth dimension between *Aguascalientia panamaensis* and the referred specimens in this paper. Adapted in part from Rincon et al. (Table 1; 2012). All measurements are in millimeters, - equals not available, APL = anterior/posterior length, TW = transverse width.

Tooth position	Specimen/ Right dentition	Specimen/ Left dentition	Range	Mean	Standard Deviation
	UOMNCH F-56354	UOMNCH F-56354			
c1 (APL)	13.69	12.69	5.16-5.68	5.324	0.205
c1 (TW)	8.66	7.39	3.68-3.90	3.81	0.083
p1 (APL)	-	8.2	5.86-7.04	6.56	0.621
p1 (TW)	-	4.74	3.52-4.06	3.85	0.289
		UOMNCH F-56352			
m1 (APL)	-	21.43	9.80-10.90	10.16	0.501
m1 (TW)	-	13.85	6.14-7.28	6.597	0.559
m2 (APL)	-	-	13.22-15.16	13.85	0.887
m2 (TW)	-	13.67	8.47-9.82	9.01	0.585
	UOMNCH F-56371				
P4 (APL)	14.32	-	7.78	7.78	-
P4 (TW)	11.80	-	8.37	8.37	-
M1 (APL)	14.92	-	10.08-12.58	11.3	1.810
M1 (TW)	15.00	-	11.18-11.96	11.57	0.551
M2 (APL)	18.65	-	13.28-14.26	13.77	0.692
M2 (TW)	18.73	-	13.75-15.11	14.43	0.962
M3 (APL)	19.13	-	13.5-14.71	14.13	0.463
M3 (TW)	17.69	-	14.67-15.74	14.87	0.598

Tribe PROTOLABIDINI Cope, 1884

Genus *TANYMYKTER* sp. Honey and Taylor, 1978

(Figs. 31-33, Table 10)

Referred Material: UOMNCH F-56313, skull with right I3, C1, P1-4, M1-3 and left P1-4, M1-3, partial right and left Ilium, from UO 4152, UOMNCH F56310, partial right maxilla with partial posterior M1 and partial M2, from UO 4152.

Description: The skull, UOMNCH F-56313 is mostly crushed dorsal ventrally (Fig. 31) but retains identifiable features.
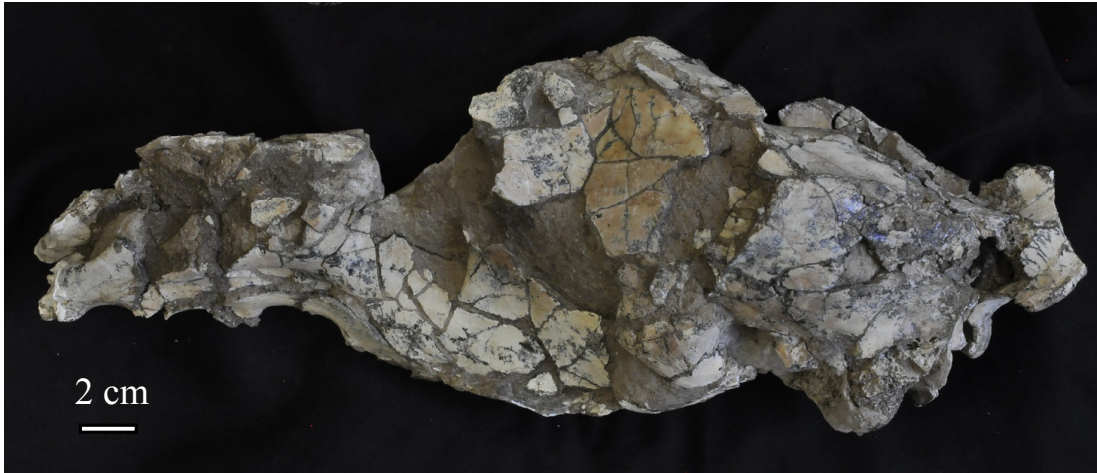
Figure 31. UOMNCH F-56313 dorsal view.

The brain case is longer than wide and the rostrum is moderately narrowed. The right I3 is robust, strongly caniniform, only slightly recurved, has a pronounced posterior ridge and is smaller than the C1. The right C1 is more recurved than the I3, larger, strongly caniniform, with a pronounced anterior and posterior ridge. The left and right P1 are moderately caniniform, markedly smaller than the I3 and C1, have strong posterior ridges and have closely appressed double roots. There are substantial diastemata between I3-C1, C1-P1 and P1-P2. The P2-P4s have strong parastyles and metastyles, and moderate mesostyles which are strongest in the P4 and less so in the P2. The lingual cingulum is notched in the P3's and not in the P4's. The M1-3's are anterioposteriorly compressed, and are wider than they are long and have a narrower waist midsection (Table 10). The parastyles, mesostyles and metastyles are stronger, increasingly from M1-M3.

The partial right maxilla of UOMNCH F-56310 (Fig. 32) is damaged. There is a partial M1 and M2, but lengths cannot be determined. The width of the M1 reported in Table 10 may be compared to UOMNCH F-56313, but the width of the M2 cannot be

59

compared; the transverse width of the posterior lobe is generally wider than the

transverse width of the anterior lobe in camelids (Honey et al., 1998).
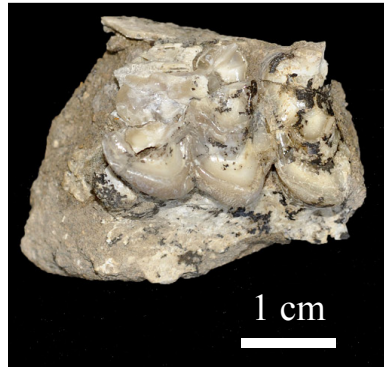
Figure 32. UOMNCH F-
56310 occlusal view.

Table 10. Dental and diastema measurements. Measurements are in millimeters, APL = anterior/posterior length, TW = transverse width, - = not available.

Tooth Position	UOMNCH F-56313		UOMNCH F-56313		UOMNCH F-56310	
	Right		Left		Right	
	APL	TW	APL	TW	APL	TW
I3	12.34	8.58	-	-	-	-
C1	14.04	11.75	-	-	-	-
P1	9.55	4.80	-	-	-	-
P1/P2 diastema	36.7		-		-	
P2	13.88	5.98	13.80	6.0	-	-
P3	15.88	8.31	15.14	8.92	-	-
P4	15.08	13.86	15.25	13.67	-	-
M1	18.70	18.89	17.49	18.79	-	19.80
M2	22.12	21.46	21.31	22.25	-	~19.75
M3	22.26	22.11	22.57	22.76	-	-

Discussion: UNMCN F-56313 (Fig. 33) can be distinguished as a protolabine by its brachyodont teeth, large, strongly caniniform I3-P1, a full complement of unreduced premolars, and a shorter cranial length relative to face length (Honey et al., 1998).

Figure 33. UOMNCH F-56313 ventral view.

Within the protolabines, it differs from its sister taxon *Protolabis* by having a molariform P4, with a strong lingual cingulum that is unbroken, C1 larger than I3, longer P1-2 diastema, anterior posteriorly shorter molars and a robust ventral tuberosity on the basisphenoid (Honey et al., 1998; Honey and Taylor, 1978). The right basisphenoid tuberosity of UNMCN F-56313 is partially broken, but the base is robust and lengthens ventrally, angled posteriorly and only slightly tapers; the left side is missing. UNMCN F-56313 differs from *Michenia* by having a caniniform C1 larger than the I3, and retention of the P1, unreduced P2-4, and shorter anterior posteriorly molars (Honey et al., 1998; Honey and Taylor, 1978). Although UNMCN F-56313 tooth dimensions (Table 10) exceed those of previously known *Tanymykter brachyodontus* (the only species as yet described), its dental morphology compares well. Honey and Taylor (1978) neither diagram nor explain how they took tooth dimensions, nor are dental measurement

conventions illustrated in other camelid literature. Terminology for camelid dentition used here is after Frick and Taylor (1968). Honey and Taylor (1978) do not define where they took their length measurements. I measured the narrowest portion of the anterior posterior length in the molars (Table 10). The widths were measured on the widest molar lobe whether it was the anterior or posterior.

UNMNCH F56310 is badly damaged and is in very late wear stage. The remaining morphology compares well to UNMCN F-56313. The M1 anterior lobe is missing, however it is possible to compare the width of the M1, as the posterior lobe of UNMCN F-56313 M1's yielded the greatest width. UNMNCH F56310's M1 is larger by a millimeter (Table 10). Of note, F56310 and F-56313 were found at the same stratigraphic level, only laterally separated by about 15 meters.

The species is not common, and has previously only been found in four formations: Vacqueros Formation (latest Arikareean-Late Hemphillian) of California, Upper Harrison Formation (latest Arikareean- Early Hemingfordian) of Wyoming and the Running Water Formation (Early Hemingfordian) of Nebraska (Honey et al., 1998).

Genus *MICHENIA* Frick and Taylor, 1971

MICHENIA Sp., Frick and Taylor, 1971

(Figs. 34-35)

Referred specimens: UOMNCH F- 56353, upper left M3, from UO 4164, UOMNCH F- 56357, anterior snout with left and right I3, left C1 and P1, anterior mandibles with left i3, left and right c1 and right p1, from UO 4155.

Description: UOMNCH F- 56353 (Fig. 34) is two-lobed, with very strong parastyle, mesostyle and metastyle, and pronounced ribs on the paracone and metacone.
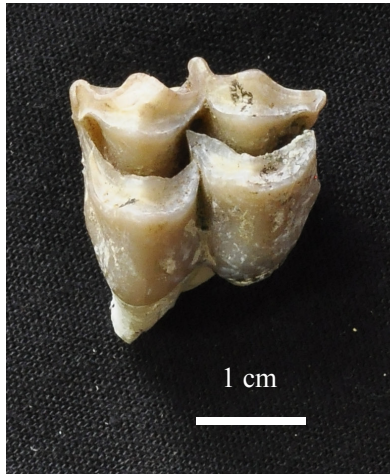

Figure 34. UOMNCH F-56353 occlusal view.

The metastyle is only slightly less prominent than the parastyle. The posterior lobe is not as wide as the anterior lobe (18.04 millimeters [mm] and 19.37 mm respectively). The molar is not strongly anterior-posteriorly shortened (length 20.04 mm). The fossettes between the labial and lingual cusps are deep. The tooth is at a early stage of wear. There is a notch separating the upper quarter of the inner and outer cusp on the posterior side of the posterior lobe. There is a cingulum on the anterior and posterior lingual cusps. On the anterior cusp it is angled from the top near the fossette to almost near the lingual base. On the posterior cusp it is not as long; it starts half way up the crown and angles down towards the fossette notch, not past it.

UOMNCH F-56357 is a partial snout and mandible. The rostrum (Fig. 35) is

markedly short with thin bones as compared to *Tanymykter* (Fig. 31). The I3, C1 and P1 are reduced and peglike as opposed to the robust caniform teeth of same position in

Figure 35. UOMNCH F-56357 snout two views. (Left) ventral view, (right) dorsal view.

Tanymykter (see above). There is a short diastema between the I3-C1 and the C1-P1.

The fused mandibles (Fig. 36) are thin with a shallow symphysis. The dorsal edge

posterior to the symphysis is sharp. The ventral surface of the posterior end of the

symphysis protrudes ventrally in a hook like projection typical of *Michenia* (Frick and

Taylor, 1971). The canines are short and caniform. The right p1 is shorter than the

canines, peglike and has a single root. The left i3 is strongly procumbent, projecting

anterior and would overlap the position of the missing i2. The mandibular foramen is just

anterior to the p1 and is slightly pocketed, not flush with the surface of the ramus.
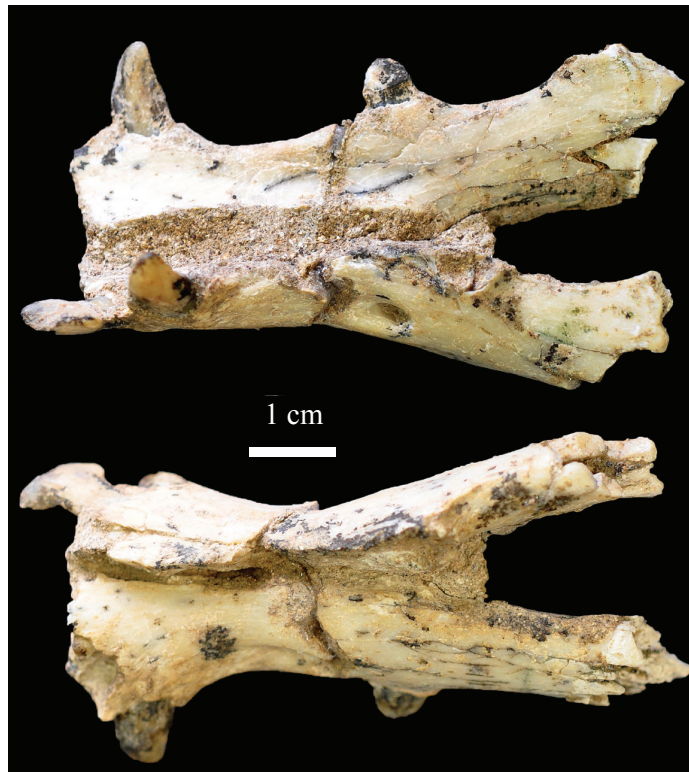

Figure 36. UOMNCH F-56357 mandibles two
views. (Top) dorsal view, (bottom) ventral view.

Discussion: UOMNCH F- 56353 can be distinguished as a protolabine by its

brachydont, two-lobed selenodont tooth morphology, unlike the stenomylines and

camelines which have higher crowned molars without parastyles, mesostyles and

metastyles as compared to protolabines. UOMNCH F-56353 is smaller (length 20.04 mm x transverse width 19.34 mm) than *Tanymykter* the only other camelid species found in the same geologic unit. In addition, the parastyle, mesostyle and metastyle are much more pronounced and the fossettes are more deeply incised in UOMNCH F-56353. The snout and mandibles of UOMNCH F-56357 were found compressed together and are assumed to be of the same individual. The upper I3's are not incisiform as in stenomylines nor are they strongly caniform as in the protolabines *Tanymykter* and *Protolabis* (Frick and Taylor, 1971; Honey et al., 1998). The snout is referable to *Michenia* (Frick and Taylor, 1971) though species cannot be determined without a more complete specimen. The mandibles are much smaller than the previously mentioned protolabines (see above). In addition, the small canines, peglike p1 and the strongly procumbent, lobed i3 with a short diastema between the i3 and c1 are indicative of *Michenia* (Frick and Taylor, 1971). *Michenia* are found throughout the continent, notably in the Upper Harrison of Wyoming (latest Arikareean) and with the Logan Mine fauna (latest Arikareean) of the Californian Great Basin (Honey et al., 1998).

Family HYPERTRAGULIDAE Cope, 1879

Genus *NANOTRAGULUS* Lull, 1922

(Fig. 37, Table 11)

Referred specimen: UOMNCH F-56306 left mandible with dentition from UO 4153.

Description: UOMNCH F-56306 (Fig. 37) is a partial left mandible missing the ascending ramus and the anterior portion forward of the p3. The mandible is short and moderately deep. The p3 is a single cusp and is shorter than the p4. The p4 is

transversely narrow and worn. The m1-m3 are worn and have strong labial protoconids and hypoconids. There is a small labial intercolumnar tubercle between the anterior and posterior lobes of the m1. The ventral portion of the posterior mandible is broken and reveals the roots of the m3. The roots extend significantly into the horizontal ramus; the molars are high crowned.

Figure 37. UOMNCH F-56306 labial view.

Discussion: UOMNCH F-56306 is a shorter, deeper and more robust mandible relative to the more elongate, slender, shallow jaws exhibited by other artiodactyls with similar morphology and similar size of teeth (Webb, 1998). It compares well to the *Nanotragulus* cf. *N. matthewi* specimens of the middle Arikareean of Texas described by Stevens et al. (1969). They describe *Nanotragulus* as having a p3 with a single cusp and an intercolumnar tubercle between the lobes of the m1 on the labial. The molar dimensions of UOMNCH F-56306 exceed the average dimensions reported by Stevens et al. (1969); comparisons are in Table 10. Stevens et al. (1969) notes that assignment to *Nanotragulus* based on tooth dimensions may not be sufficient since most share very similar tooth morphology but are slightly dissimilar in size. I assign UOMNCH F-56306

to *Nanotragulus* based on tooth characters though its tooth dimensions slightly exceed *N.*

matthewi reported by Stevens et al. (1969).

Table 11. Dental measurements for UOMNCH F-56306. Comparison of UOMNCH F-56306 tooth dimensions to that of the maximum tooth dimensions of Stevens et al. (1969; Table 8). Measurements are in millimeters, APL = anterior/posterior length, TW = transverse width, - = not available.

Tooth Position	*Nanotragulus* cf. *N. matthewi*		UOMNCH F-56306	
	APL	TW	APL	TW
p3	-	-	2.22	1.80
p4	-	-	7.80	2.89
m1	6.6	4.4	7.96	5.96
m2	7.3	4.2	9.03	6.80
m3	10.0	4.1	13.93	6.80

Family MOSCHIDAE Gray, 1821

Subfamily BLASTOMERYCINAE Frick, 1937

Genus *BLASTOMERYX* Cope, 1877

(Figs. 38-40)

Referred specimens: UOMNCH F-56348, left partial dentary with m1, m2 from

UO4152, UOMNCH F-56360, right partial dentary with partial p2, p3, p4, m1 from

UO4155, UOMNCH F-56390, left partial dentary with partial m2, m3 from UO4164

Description: The left dentary of UOMNCHF-56348 (Fig. 38) is shallow and thin. Both

molars have strong protoconids and hypoconids that form V-shaped crescents on the

labial side, with small intercolumnar tubercules between each molars anterior and

posterior lobes (on labial side). The fossettes are moderately deep.   The paraconids, metaconids and entoconids are weak while the entostylid is strong.
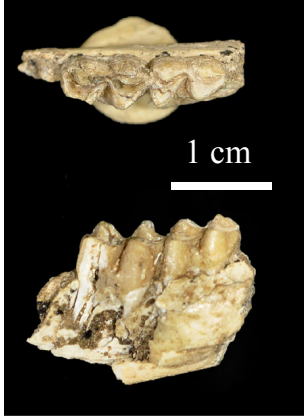

Figure 38. UOMNCH F-56348 two views. (Top) occlusal view, (bottom) labial view.
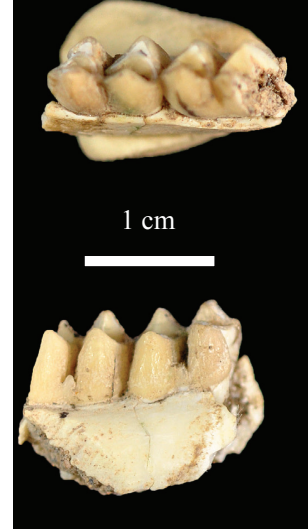
Figure 39. UOMNCH F-56390 two views. (Top) occlusal view, (bottom) labial view.

The molars of UOMNCH F-56390 (Fig. 39) are very similar UOMNCH F-56348.   The m2 and m3 of UOMNCH F-56390 have strong intercolumnar tubercles that are characteristic of this genus (Frick, 1937; Webb, 1998). The partial horizontal ramus of UOMNCH F-56360 is slender and shallow. The p2 is broken off almost to the base and is reduced relative to p3. The p3 and p4 paraconulid and hypoconulid are subequal due to wear and the metaconid is more prominent. They are slightly lobed on the labial side and not on the lingual as in the m1. The m1 shows a late wear stage and is worn smooth, cupped labial and lingually, to the dorsal edge of the intercolumnar tubercle.
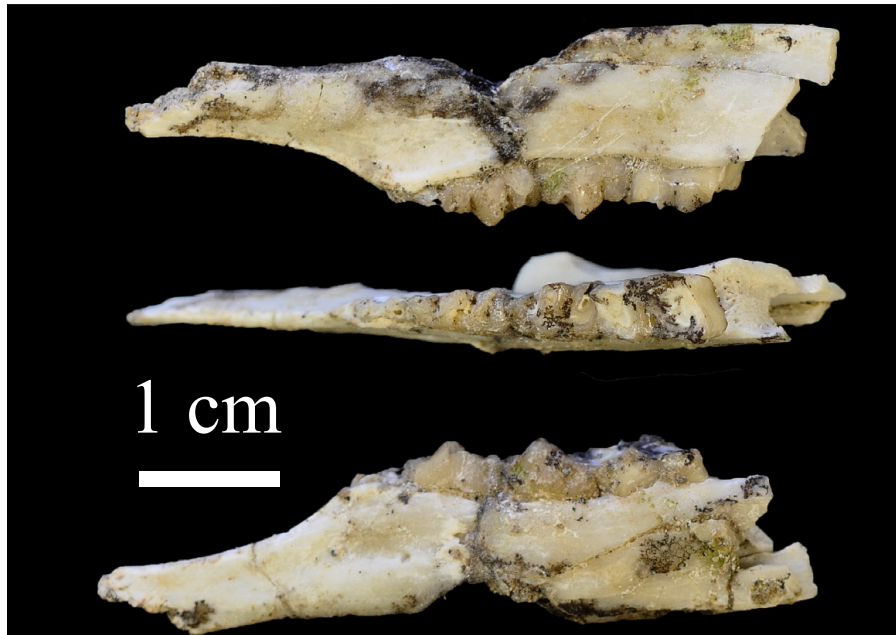
Figure 40. UOMNCH F-56360 three views. (Top) labial view, (middle) occlusal view, (bottom) lingual view.

Discussion: Differences in tooth dimension and placement of mandibular fossa in these small selenodont ruminants seem to vary regionally (Frick, 1937 and Webb, 1998). *Blastomeryx* sp. is fairly ubiquitous across the continent and temporally from the latest Arikareean through late Clarendonian (Webb, 1998). Tedford et al. (2004) considers it to be part of a typical latest Arikareean assemblage in the physiogeographic province of the northern Rocky Mountains. The moschids have not had a modern revision in some time therefore assignment to species without more complete specimens would be dubious at best. However, the tooth morphology and ratios established by Frick (1937) make the assignment of UOMNCH F-56360 to the genus possible as the ratios suggest *B. gemmifer* as a likely identity. In UOMNCH F-56360, the p2/p4 ratio of 73% falls within Frick's

(1937) range of 73-80% and the p3/p4 of 97% is not unreasonable given the range 93-95%; both for *B. gemmifer*. Each of the three specimens shares at least one tooth position with another; those shared teeth appear identical. The UO localities 4152, 4155 and 4164 in which the specimens were found are all in the same lithologic unit Ss1 (Figures 9, 10). UOMNCH F-56348 and UOMNCH F-56360 were found *in situ*.

Additional Faunal List

I have listed the following species found at Coglan Buttes. Though I have not fully

described these as yet, they are of use to aid in my discussion of the fauna's affinity to

other North American fossil localities. All of the rodents except for the *Mylagaulodon*

are represented by isolated cheek teeth. Additional comparison and study of them will

have to take place before they can be formally described.

Squamata
Lagomorpha
      Ochotonidae
      Leporidae
Rodentia
      Aplodontidea
         Aplodontidae
            Allomys
            Meniscomys
         Geomyidae
            Entoptychinae
               Pleurolicus
               Entoptychus
         Cricetidae
            Leidymys
Artiodactyla
      Promerycochoerinae
      Hypertragulid
Perrisodactyla
      Equidae
         Mesohippus
         Archaeohippus
         Kalobatippus
      Chalicotheroidea
         Moropus
      Rhinocerotoidea

Discussion of Assemblages

The faunal assemblages of Coglan Buttes show distinct change throughout the various geologic units. Lowest in the section at Guzzler, localities UO 4184 and UO 4166 (Fig. 4) produced *Leptocyon*, a larger canid, *Hypertragulus, Mesohippus, Leidymys, Allomys*, oreodonts and rhinocerotids. No other identifiable material was found between these sites and the Paisley tuff. The first geologic unit (Ss1) above the Paisley tuff, is the most productive in the area. *Osbornodon iamonensis, Paracynarctus, Tanymykter, Michenia, Blastomeryx, Moropus, Kalobatippus, Archeohippus, Leidymys, Allomys Meniscomys* and *Pleurolicus,* and various lagomorphs are found in localities UO 4152 (Fig. 6), UO 4164-5 and UO 4155-6 (Fig. 5) of the Ss1 geologic unit. Stratigraphically above the first pyroclastic deposit (Tp1), the second massive sandstone unit (Ss2) is also productive but not in the vicinity of Beardog or Shelter sections. The faunal assemblage found in this unit comes from the Mylagaulid area only. Ss2 has produced *Mylagaulodon, Aguascalientia,* oreodonts and various lagomorphs from localities UO 4158, UO 4162-3 (Fig. 7). Highest in the stratigraphy, the Ss4 (Fig. 6) has only produced one identifiable specimen, *Nanotragulus* from UO 4153.

Comparing the Coglan Buttes assemblages to that of the John Day Basin (JDB) faunas is necessary; the two are closer in proximity than to other faunas of the earliest Miocene. The Arikareean intervals of the JDB were not well understood until recent work by Hunt and Stepleton (2004) and later by Albright et al. (2008). Albright et al. (2008) revised the chronostratigraphy of over 500m of stratigraphic section across 300 sites, calibrating the magnetostratigraphy with several radiometrically dated tuffs. Comparing

72

the JDB with the Great Plains Arikareean does not help to clarify faunal differences in the John Day. The latest Arikareean is not well defined in the Great Plains where the NALMA age was first typified (Woodburne, 2004). The Great Plains Arikareean units are discontinuous, bounded by significant unconformities, faunal hiatuses and poor paleomagnetic records to aid chronostratigraphy (Albright et al, 2008). Albright et al.'s (2008) and Hunt and Stepleton's (2004) latest revisions provide the best comparison to reach an age estimate for Coglan Buttes fauna.

Leptocyon, Allomys, Mesohippus and *Leidymys* have been found in the Turtle Cove Member (TCM) of the John Day Formation that is early Arikareean (Albright et al., 2008). This suggests that at least the lowest fossil producing units of the Guzzler section is at the least Arikareean (30-19.4 Ma).

The fauna from Coglan Buttes Ss1 geologic unit shares similarities with several members in the John Day Basin. *Allomys* is found throughout units E-K (lower to upper) of the TCM (Albright et al., 2008). *Meniscomys* and *Pleurolicus* are found within G-J of the TCM (Albright et al., 2008). *Entoptychus* and *Leidymys* have been found in the Kimberly Member in units K-M (Albright et al., 2008). All of the microfauna named previously are rodents. Of the macrofauna found within the Ss1 of Coglan Buttes, only a few are also found in the John Day Basin. The equid *Kalobatippus* is found in the Kimberly, Haystack Valley, Balm Creek, Johnson Canyon and Rose Creek Members and range from middle Arikareean to earliest Hemingfordian, respectively (Albright et al., 2008; Hunt and Stepleton, 2004). *Moropus*, a chalicothere, is found in unit M of the Kimberly Member (middle Arikareean) through earliest Hemingfordian of the Rose Creek Member (Albright et al., 2008; Hunt and Stepleton, 2004). *Archeohippus* has only

been found in the Johnson Canyon Member, spanning the late Arikareean (Albright et al., 2008; Hunt and Stepleton, 2004).

The Ss2 of Coglan Buttes has *Mylagaulodon* in common with the Johnson Canyon (Arikareean) and Rose Creek Members (latest Arikareean-earliest Hemingfordian) of the JDM (Hunt and Stepleton, 2004). Though Ss2 also contains lagomorphs, none have been described as yet. Further work may find that Coglan Buttes also shares lagomorphs in common with the JDM.

The uppermost geologic unit of Coglan Buttes that has produced identifiable specimens is the Ss4. A specimen of *Nanotragulus* was found in the unit. *Nanotragulus planiceps* has been found in units E-J of the TCM. I compare the Coglan Buttes *Nanotragulus* to that of the Texan *Nanotragulus matthewi* based on tooth morphology. The Texan specimens of Stevens et al. (1969) are from late Arikareean deposit.

CHAPTER IV

DISCUSSION

Much of the general importance of the Coglan Buttes fauna revolves around what can be said about the most fossiliferous layers Ss1 and Ss2, both above the Paisley tuff. The Ss1 does share species in common with the John Day Formation. Importantly, the shared species indicate an Arikareean age for the Ss1. It is interesting that the Ss1 layer of Coglan Buttes contains species that are fairly geographically and temporally restricted to separate members in the John Day Basin. Species such as *Meniscomys* and *Pleurolicus* are fairly restricted both stratigraphically and temporally. While the rodent population of Coglan Buttes Ss1 suggests a late Arikareean age, some of the macrofauna does not. *Moropus, Kalobatippus* and *Archeohippus* do extend into the latest Miocene elsewhere in the country (Carrasco et al., 2005).

More interesting, the Ss1 of Coglan Buttes contains late Arikareean camelids (*Tanymykter* and *Michenia*) and canids (*Osbornodon iamonensis* and *Paracynarctus*) not found in the John Day Basin, but in many of the southern United States. While Coglan Buttes does not share any camelids in common with the John Day Formation, it is worth mentioning that both places lack the high crowned stenomylines that are often found in Arikareean deposits elsewhere (McKenna, 1966). The canids of the Ss1 unit do not aid in determining an age assignment; both canids are found throughout most of the Miocene. Both camelids (*Michenia* and *Tanymykter*) and the canid (*Osbornodon iamonensis*) of the Coglan Buttes Ss1 are first records of the species for Oregon (Carrasco et al., 2005).

A suggested age for the Ss2 of Coglan Buttes is not clear as yet. Unfortunately,

75

only the outcrops in the Mylagaulid area produce fossils from this stratigraphic unit. *Aguascalientia* suggests a latest Arikareean age. Of note, this record of *Aguascalientia* is the furthest north documented to date; previously it was known from the latest Arikareean of Texas and Florida (Rincon et al, 2012 and Honey et al, 1998). This is consistent with the finding that the assemblage downsection in the Ss1 unit also demonstrates a southern latitude affinity. While *Aguascalientia* suggests a latest Arikareean age for Ss2, *Mylagaulodon* is not restricted to the Arikareean. A pending radiometric date for the capping pyroclastic unit (Tp2) will determine the age for the Ss2.

The age of the uppermost fossil-producing unit of the Ss4 cannot be determined as yet. Though *Nanotragulus* has not been found past the latest Arikareean (Carrasco et al., 2005) the age cannot be determined based on one specimen.

Since the faunal assemblages above Guzzler suggest possibly a middle to latest Arikareean age, it follows that the localities down section will be at least middle Arikareean. The canid (*Leptocyon)* from the Guzzler area is fairly widespread, both temporally and geographically; so it does not aid in determining an age for the lowest fossiliferous beds.

The geology of Coglan Buttes area is quite different from that of the age-equivalent John Day Basin. While both areas contain numerous tuffs, they record very different depositional environments. The thick paleosol units of the John Day Basin indicate well-watered habitat and long term soil formation (Retallack et al., 2000) while the debris flows, pyroclastic deposits and tuffs of Coglan Buttes likely indicate a more quickly-changing landscape and significant paleotopography that formed close to active volcanic centers.

CHAPTER V

CONCLUSIONS

In light of the above discussion, it is apparent that most of the assemblages of Coglan Buttes are Arikareean. Paleontologists have long recognized that the faunas of Oregon show distinct local zoogeography (Shotwell, 1961; Woodburne, 2004), especially throughout the Miocene and later. In addition, Woodburne (2004) notes that the southern latitude faunas of New Mexico and Texas also exhibit local endemism in the early Miocene. Strict comparison to the John Day Basin assemblages or the southern assemblages would not serve to elucidate an age for Coglan Buttes before radiometric dates are obtained. That Coglan Buttes faunas share an affinity with the John Day Basin, the southern localities and the Great Plains indicates an even greater opportunity to investigate the timing of biotic exchange, as was done by Albright et al (2008) for the John Day Basin. Additionally, in light of the affinity Coglan Buttes Fauna shares with both the John Day Basin and southern North America, future paleomagnetic chronology studies, additional radiometric dates and continued fossil collection and description of the Coglan Buttes area will serve to serve to illuminate a time period for which the terrestrial mammal record is not well-known elsewhere in North America (Woodburne, 2004).

The affinity that some of the Coglan Buttes faunas share with more southern latitudes assemblages suggests a more sub-tropical environment than the John Day Basin. Furthermore the southern affinity of the macrofauna suggests that geographic barriers were not a factor in the faunal exchange between Coglan Buttes and elsewhere in the continent.

The geology of Coglan Buttes reveals an interesting contrast to depositional environments of the John Day Basin. Prior to deposition of the Paisley tuff, the area was most likely fluvial dominated as indicated by the numerous reworked, lightly bedded units. The entire lowest part of the immediate basin appears to have been infilled gradually. Gentle topography is suggested by laterally subequal bedding.

After the deposition of the Paisley tuff, the thick debris flow and pyroclastic deposits eventual infilling of the basin. Flood basalts and dacites that cap the entire section, visible throughout the region may indicate the last of the Miocene deposition events. The over 440 m of sedimentary and volcanic deposits thin toward the north and south margins of the study area. This confirms Scarberry's et al., (2009) suggestion that substantial early Miocene paleotopography existed prior to Basin and Range extension.

A more accurate age estimate of earliest Miocene (Arikareean) for most of the fossil assemblages and lithologic units has been demonstrated in this paper. Future work will provide a better understanding of Oregon in earliest Miocene time, both geologically and paleontologically.

REFERENCES CITED

Albright III, L. B., M. O. Woodburne, T. J. Fremd, C. C. Swisher III, B. J. MacFadden, and G. R. Scott. 2008. Revised Chronostratigraphy and Biostratigraphy of the John Day Formation (Turtle Cove and Kimberly Members), Oregon, with Implications for the Updated Calibration of the Arikareean North American Land Mammal Age. Journal of Geology 116 (3):211-237.

Branney, M. J., and P. Kokelaar. 2002. Pyroclastic Density Currents and the Sedimentation of Ignimbrites. Geological Society, London, Memoirs, (27):1-143.

Carrasco, M. A., B. P. Kraatz, E. B. Davis, and A. D. Barnosky. 2005. Miocene Mammal Mapping Project (MIOMAP). University of California Museum of Paleontology. Available at: www.ucmp.berkeley.edu/miomap.

Coombs, M. C., and W.P. Coombs, Jr. 1997. Analysis of the Geology, Fauna, and Taphonomy of Morava Ranch Quarry, Early Miocene of Northwest Nebraska. Palaios 12:167-187.

Fremd, T. J. 2010. Guidebook: SVP Field Symposium 2010, John Day Basin Field Conference. Geoscientists-in-the-Parks document, 2009-GRD. National Park Service, Denver, CO.

Flynn, L. J., and L. L. Jacobs. 2008. Aplodontoidea; pp. 377-390, in C. V. Janis, G. F. Gunnell, and M.D. Uhen (eds.), Evolution of Tertiary Mammals of North America. Volume 2: Small Mammals, Xenarthrans, and Marine Mammals. Cambridge University Press, Cambridge.

Frick, C., and B. E. Taylor. 1968. A Generic Review of the Stenomyline Camels. American Museum Novitates (2353):1-51.

Frick, C. and B.E. Taylor. 1971. *Michenia*, a New Protolabine (Mammalia, Camelidae) and a Brief Review of the Early Taxonomic History of the Genus *Protolabis*. American Museum Novitates (2444):1-24.

Honey, J. G., and B. E. Taylor. 1978. A Generic Revision of the Protolabidini (Mammalia, Camelidae), With A Description of Two New Protolabidines. Bulletin of the American Museum of Natural History 161(3): 369-425.

Honey, J. G., J. A. Harrison, D.R. Prothero, and M.S. Stevens. 1998. Camelidae; pp.439-462, in C.M. Janis, K.M. Scott, and L.L. Jacobs (eds.), Evolution of Tertiary Mammals of North America. Volume 1: Terrestrial Carnivores, Ungulates, and Ungulate like Mammals. Cambridge University Press, Cambridge.

Huggel, C. 2008. Recent extreme slope failures in glacial environments: effects of thermal perturbation. Quaternary Science Reviews. Available at: doi:10.1016/j.quascirev.2008.06.007.

Hunt, R. M., Jr. 2011. Evolution of Large Carnivores During the Mid-Cenozoic of North America: The Temnocyonine Radiation (Mammalia, Amphicyonidae). Bull. of the American Museum of Natural History (358):1-153.

Hunt, R. M., Jr., and E. Stepleton. 2004. Geology and Paleontology of the Upper John Day Beds, John Day River Valley, Oregon: Lithostratigraphic and Biochronologic Revision in the Haystack Valley and Kimberly Areas (Kimberly and Mt. Misery Quadrangles). Bulletin of the American Museum of Natural History (282):1-90.

Korth, W. W. 1994. The Tertiary record of rodents in North America. Topics in Geobiology 12:319. Plenum Press, New York.

Korth, W. W. 1999. *Hesperogaulus*, A New Genus of Mylagaulid Rodent (Mammalia) from the Miocene (Barstovian to Hemphillian) of the Great Basin. Journal of Paleontology 73:945-951.

Korth, W. W. 2000. Review of Miocene (Hemingfordian to Clarendonian) Mylagaulid Rodents (Mammalia) from Nebraska. Annals of Carnegie Museum 69:227-280.

Lawrence, J. F., and L. L. Jacobs. 2008. Aplodontoidea; pp.377-390, in C. M. Janis, G. F. Gunnell, and M. D. Uhen (eds.), Evolution of Tertiary Mammals of North America. Volume 2: Small Mammals, Xenarthrans, and Marine Mammals. Cambridge University Press, Cambridge.

Matthew, W. D., and J. R. MacDonald. 1960. Two New Species of *Oxydactylus* from the Middle Miocene Rosebud Formation in Western South Dakota. American Museum Novitates (2003):1-7.

McKenna, M. C. 1966. Synopsis of Whitneyan and Arikareean Camelid Phylogeny. American Museum Novitates (2253):1-11.

Meigs, A., K. Scarberry, A. Grunder, R. Carlson, M. T. Ford, M. Fouch, T. Grove, W. K. Hart, M. Iademarco, B. Jordan, J. Milliard, M. J. Streck, D. Trench, and R. Weldon. 2009. Geological and geophysical perspectives on the magmatic and tectonic development, High Lava Plains and northwest Basin and Range. Field Guides 15:435-470.

Munthe, K. 1989. The skeleton of the Borophaginae (Carnivora: Canidae). University of California Publications in Geological Sciences 133:1–115.

Peterson, N. V. 1959. Preliminary Geology of the Lakeview Uranium Area, Oregon: Oreg. Dept. Geology and Min. Ind., Ore Bin 21:11-16.

Peterson, N. V., and J. R. McIntyre. 1970. The Reconnaissance Geology and Mineral Resources of Eastern Klamath County and Western Lake County, Oregon: Oreg. Dept. Geology and Mineral Industries, Bulletin 66:1-70.

Rasband, W. S., ImageJ, U. S. National Institutes of Health, Bethesda, Maryland, USA, Available at: http://imagej.nih.gov/ij/, 1997-2012.

Renne, P. R., A. L. Deino, R. C. Walter, B. D. Turrin, C. C. Swisher III, T. A. Becker, G. H. Curtis, W. D. Sharp, and A. R. Jaouni. 1994. Intercalibration of astronomical and radioisotopic time. Geology 22:783-786.

Retallack, G. J., E. A. Bestland, and T. J Fremd. 2000. Eocene and Oligocene paleosols of central Oregon. Geological Society of America, Special Paper 344:1–192.

Rincon, A. F., J. I. Bloch, C. Suarez, B. F. MacFadden, and C. A. Jaramillo. 2012. New Floridatragulines (Mammalia, Camelidae) from the Early Miocene Las Cascadas Formation, Panama. Journal of Vertebrate Paleontology 32:456-475.

Scarberry, K. C., A. J. Meigs, and A. L. Grunder. 2009. Faulting in a Propagating Continental Rift: Insight from the late Miocene structural development of the Abert Rim Fault, southern Oregon, USA. Techtonophysics. Available at: doi:10.1016/j.tect.2009.09.025.

Shotwell, J. A. 1961. Late Tertiary Biogeography of Horses in the Northern Great Basin. Journal of Paleontology 35:203-217.

Sinclair, W. S. 1903. *Mylagaulodon*, a new rodent from the Upper John Day of Oregon. American Journal of Science 15:143-144.

Stevens, M. S. 1977. Further Study of Castolon Local Fauna (Early Miocene) Big Bend National Park, Texas. The Pearce-Sellards Series (28):1-69.

Stevens, M. S., J. B. Stevens, and M. R. Dawson. 1969. New Early Miocene Formation and Vertebrate Local Fauna, Big Bend National Park, Brewster County, Texas. The Pearce-Sellards Series (15):1-53.

Stromberg, C. A. E. 2004. Using phytolith assemblages to reconstruct the origin and spread of grass-dominated habitats in the Great Plains of North America during the late Eocene to early Miocene. Palaeogeography, Palaeoclimatology, Palaeoecology 207:239-275.

Tedford, R. H., L. B. Albright III, A. D. Barnosky, I. Ferrusquia-Villafranca, R. M. Hunt Jr., J. E. Storer, C. R. Swisher III, M. R. Voorhies, S. D. Webb, and D. P. Whistler. 2004. Mammalian biochronology of the Arikareean through Hemphillian interval (late Oligocene through early Pliocene epochs), pp. 169-231, In Woodburne, M.O. (ed.), Late Cretaceous and Cenozoic Mammals of North America: Biostratigraphy and Geochronology. Columbia University Press, New York.

Tedford, R. H., X. Wang, and B.E. Taylor. 2009. Phylogenetic Systematics of the North American Fossil Caninae (Carnivora: Canidae). Bulletin of the American Museum of Natural History (325):218.

Van Valkenburgh, B. 1991. Iterative evolution of hypercarnivory in canids (Mammalia: Carnivora): evolutionary interactions among sympatric predators. Paleobiology 17:340-362.

Walker, G. W., U. S. Geological Survey. Reconnaissance Geologic Map of the Eastern Half of the Klamath Falls (AMS) Quadrangle, Lake and Klamath   Counties, Oregon. [map]. Version 1. 1:250,000. Mineral Investigations Field Studies Map; MF-260. U.S. Department of the Interior, USGS, 1963.

Wang, X. 1993. Transformation from plantigrady to digitigrady: functional morphology of locomotion in *Hesperocyon* (Canidae: Carnivora). American Museum Novitates 3069:1-23.

Wang, X. 1994. Phylogenetic Systematics of the Hesperocyoninae (Carnivora: Canidae). Bulletin of the American Museum of Natural History 221:1-212.

Wang, X. 2003. Chapter 8: New Material of *Osbornodon* from the Early Hemingfordian of Nebraska and Florida. Bulletin of the American Museum of Natural History 279:163-176.

Wang, X., R. E. Tedford, and B. E. Taylor. 1999. Phylogenetic systematics of the Borophaginae (Carnivora: Canidae). Bulletin of the American Museum of Natural History 243:1–39.

Webb, S. D. 1998. Hornless ruminants; pp. 463-476, In C. M. Janis, K. M. Scott, and L. L. Jacobs (eds.), Evolution of Tertiary Mammals of North America. Volume 1: Terrestrial Carnivores, Ungulates, and Ungulatelike Mammals. Cambridge University Press, Cambridge.

Wilson, J. A., 1960. Miocene Carnivores, Texas Coastal Plain. Journal of Paleontology 34:983-1000.

Wilson, J. A., 1974. Early Tertiary Vertebrate Faunas, Vieja Group and Buck Hill Group, Trans-pecos Texas: Protoceratidae, Camelidae, Hypertragulidae. Texas Memorial Museum Bulletin 23:1-34.

Woodburne, M. O., 1998. Arikareean and Hemingfordian faunas of the Cady Mountains, Mojave Desert Province, California. In, Depositional environments, lithostratigraphy and biostratigraphy of the White River and Arikaree groups (late Eocene to early Miocene, North America), ed. D.O. Terry Jr., H.E. LaGarry, and R.M. Hunt Jr. Geological Society of America Special Paper 325: 197-210.

Woodburne, M.O. 2004a. Principles and Procedures; pp. 1-20 In M.O. Woodburne (ed.), Late Cretaceous and Cenozoic mammals of North American: Biostratigraphy and geochronology. Columbia University Press, New York.

Woodburne, M.O. 2004b. Global events and the North American mammalian biochronology; pp. 315-345, In M.O. Woodburne (ed.), Late Cretaceous and Cenozoic mammals of North American: Biostratigraphy and geochronology. Columbia University Press, New York.